WAVELENGTH DEPENDENCE OF THE POLARIZATION OF LIGHT REFLECTED FROM A PARTICULATE SURFACE IN THE SPECTRAL REGION OF A TRANSITION METAL ABSORPTION BAND

by

Carle E. Pieters

B.A., Antioch College
(1966)

S.B., Massachusetts Institute of Technology
(1971)

SUBMITTED IN

PARTIAL FULFILLMENT OF THE REQUIREMENTS FOR THE

DEGREE OF MASTER OF SCIENCE

at the

MASSACHUSETTS INSTITUTE OF TECHNOLOGY

September, 1972

Department of Earth and Planetary Sciences, August 14, 1972

Certified by: _____

Thesis Supervisor

Accepted by: _____

Chairman, Departmental Committee on Graduate Students

Wavelength Dependence of the Polarization of Light Reflected from a Particulate Surface in the Spectral Region of a Transition Metal Absorption Band

by
Carle E. Pieters

Submitted to the
Department of Earth and Planetary Sciences
August 1972
in partial fulfillment of the requirements for the
degree of Master of Science

ABSTRACT

A theoretical and experimental study was undertaken to examine the polarimetric properties of particulate surfaces in the spectral region (.7 to 1.1 microns) of a mineral absorption band. The purpose of the investigation was to show that spectral polarimetry is an alternative diagnostic tool to absolute reflectivity measurements for some applications, notably the determination of absorption band positions for the lunar surface.

The major results are: 1) Polarization increases significantly in an absorption band at high phase angles. 2) The amount of increase is dependent on particle size as well as amount and type of minerals it is mixed with. 3) Although the percent change of polarization in an absorption band is greater for transparent mixtures, the magnitude of change of polarization is greater for mixtures with absorbing menerals. 4) The maximum of the polarization variation corresponds directly with the center of the absorption band.

These variations are interpreted to be due to the changing ratio of specular to diffuse components of light reflected from a particulate surface.

Thesis Supervisor: Thomas B. McCord
Title: Associate Professor of Planetary Physics

Table of Contents

ACKNOWLEDGEMENTS

It would be impossible to mention all the people who in some way have been a help (or a hindrance) in completing this project. A special disappointment were Massachusetts meteorologists (although it wasn't their fault). I am very fortunate to have a warm husband, Ned, who consoled me many times in the face of cloudy skies and equipment failures and other things.

I would especially like to thank Dr. Tom McCord not only for the helpful discussions we've had, but also for his patience as I worked in his lab while so many other projects needed tending to. I am grateful to Dr. Roger Burns for the use of his Cary 17 spectrometer, for many informative discussions, and for the encouragement he gave to continue the project. I am indebted to Earl Whipple and Jim Besancon for their assistance in obtaining samples. I would like to thank Rateb Abu-Eid for introducing me to the Cary and for rescuing me from some hoodlums while working late one night. I would like to thank Jay Elias, Mike Gaffey, and Larry Lebofsky of MITPAL for the many discussions we've had while I've been playing with the ideas. I am thankful for the tollerance of all the members of MITPAL whom I deprived of cokes and lunches while I was working in the Lurker's Den.

I. Preface

A readily accessible source of information about planetary objects of our solar system is the light reflected by them. When light is reflected by a surface it is altered in a way dependent promarily upon the composition and structure of the surface. By knowing the properties of the light source (the sun), and how the variables of composition and structure affect the reflection of light, one can interpret the reflected light from a planetary object in terms of its surface composition and structure.

Light reflected from a nonopaque particulate surface, such as the surface of the moon, contains a component that has been transmitted through the particles. Transmission features of the surface material are thus evident in a reflection spectrum. Some of the most useful compositional information available in a reflection spectrum are well defined absorption bands in the visible and near infrared spectral region caused by transition elements (Fe, Ti, Cr, etc.) in crystal structures of various common silicate minerals.

One can detect these absorption features, and thus partially identify the composition of the surface, by using earth-based telescopes to measure the reflected light. It is necessary to concurrently measure the object and a star in a similiar position in the sky to eliminate atmospheric and equipment effects. By calibrating the observed star with the sun, one can obtain the object's reflectivity, the ratio of the reflected

light to the incident light. This technique has been particularly successful in interpreting the lunar surface and has been verified by Apollo sampling. (See references by Adams and McCord.)

It was hypothesized that not only would an absorption band (if it existed) appear in the measured reflectivity of an object, but it would also be evident in spectral polarimetric measrurments (the measured polarization of the reflected light at different wavelengths). The basis for this hypothesis came from pieces of reported polarimetric and spectral reflectivity studies of terrestial and lunar material. A preliminary laboratory invistigation undertaken in 1971 (unpublished) showed that at large phase (100°) there is indeed preferential absorption in one polarized component of the reflected light, causing an increase in polarization in an absorption band.

This effect could be useful for an independent, and perhaps simpler, technique for detecting absorption bands in a telescopically measured reflection spectrum. It would allow the observer to directly compare components of reflection to detect an absorption rather than the multi-step procedure to measure the absolute reflectivity.

The study presented here was undertaken to define and clarify this spectral polarimetric effect with crystal field absorption bands, and to later apply it to telescopic observations. The program originally contained three parts: 1) a theoretical examination of the implications of Fresnel's equations of

reflection in the region of a crystal field absorption band, 2) a laboratory investigation of the polarization properties of reflected light from known samples in the region of a crystal field absorption, and 3) telescopic observations of areas on the moon to identify absorption bands using polarimetric techniques. The first two of these are presented here. Telescopic observations are now in process and will be completed in the near future.

II. Background

This section is a brief report and description of equations and information essential to the discussion of the next sections. The units used throughout this paper are MKS units unless otherwize stated.

A. Characteristic Absorption Features of Minerals: Crystal Field Theory

Absorption features in the visible and near infrared spectral region of transmitted light for common rock forming minerals have been studied extensively and can be readily explained by crystal field theory considerations. (Burns) The absorption bands of the spectrum in this region are generally d-d orbital electron transitions of transition metal ions (Fe, Cr, Ti, Ne, etc.) whose d orbital energy levels are no longer degenerate but have been split due to the effect of the negative ions, ligands, around them in the crystal lattice. The magnitude of this energy level split, and thus the wavelength of the energy absorbed to make the transition, is strongly dependent on the transition metal ion, the crystal environment, and the metal-ligand distance. Distortion of the symmetry of the crystal site causes more complex splitting and more than one crystal field absorption band.

The width of an absorption band from d-orbital transitions is governed by the lattice vibrations of the crystal. Since the wavelength dependence of the absorption is strongly affected by the metal-oxygen distance of the silicate, the

slight variations of this distance caused by the vibrations creates an absorption band with a gaussian distribution of absorptions. The observed bandwidth is this gaussion centered on the resonant frequency associated with the mean metal-oxygen distance.

Other absorption features evident in a transmission spectrum of a silicate are those caused by charge transfer transitions between neighbouring metal ions or between metal-oxygen ions. These absorptions are generally intense and are the primary cause for the absorption edge of silicates in the ultraviolet.

By combining crystal field theory and empirical measurements on well known silicate minerals, features of a transmission spectrum can be well defined and classified allowing transmission spectra to be used as a diagnostic tool.

A notable characteristic of the absorption transition is that the probability of interaction between an electron and a photon of the correct energy is also dependent on the orientation of the orbitals, governed by the crystal lattice, and the direction of propagation of radiation. These absorption differences are defined by measuring polarized spectra along different crystalographic axes. (see Burns) A reflection spectrum, however, includes a summation of light from randomly oriented crystals. The angular dependence information is lost, making reflection spectra a slightly more complex diagnostic tool.

B. Fresnel's Equations and Related Topics

Reflection from and transmission through a dielectric surface can be described theoretically by Fresnel's equations, which can be expressed using Snell's law as:

$$\eta = \frac{\sin\theta}{\sin\varphi} \qquad \text{Snell's law} \qquad \text{II.1}$$

$$R_{\perp} = \left| \frac{\cos\theta - \sqrt{\eta^2 - \sin^2\theta}}{\cos\theta + \sqrt{\eta^2 - \sin^2\theta}} \right|^2 \qquad \text{II.2}$$

Reflection

$$R_{\parallel} = \left| \frac{\eta^2\cos\theta - \sqrt{\eta^2 - \sin^2\theta}}{\eta^2\cos\theta + \sqrt{\eta^2 - \sin^2\theta}} \right|^2 \qquad \text{II.3}$$

$$T_{\perp} = \left| \frac{2\cos\theta}{\cos\theta + \sqrt{\eta^2 - \sin^2\theta}} \right|^2 * TK \qquad \text{II.4}$$

Transmission

$$T_{\parallel} = \left| \frac{2\eta\cos\theta}{\eta^2\cos\theta + \sqrt{\eta^2 - \sin^2\theta}} \right|^2 * TK \qquad \text{II.5}$$

where $TK = \frac{\eta\cos\varphi}{\cos\theta} = \left| \frac{\sqrt{\eta^2 - \sin^2\theta}}{\cos\theta} \right|$

θ is the angle of incidence

φ is the (complex) angle of refraction

$R_{\parallel}$ and $T_{\parallel}$ are in the plane of scattering (containing the incident and reflected vectors)

$R_{\perp}$ and $T_{\perp}$ are perpendicular to the plane of scattering

η is the (complex) refractive index.

The <u>phase angle</u> α is the angle between the incident vector and reflected vector.

Figures II.1 and II.2 show how the two components of the specular reflection vary with phase for the real refractive index $\eta = 1.5$ and $\eta = 1.7$. Also shown in the figures is the computed polarization P for the reflected light where the percent polarization is defined as:

$$P = \frac{I_{\perp} - I_{\parallel}}{I_{\perp} + I_{\parallel}} \times 100 \qquad \text{where I is intensity.} \qquad \text{II.6}$$

The derivation of Fresnel's equations as well as Snell's law from Maxwell's equations, the wave equation solution, and boundary conditions can be found in most optics books. (Born, Garbuny, Fowles)

Note that at the dielectric boundry in the above equations reflection and transmission account for all the light, ie. R+T=1. When absorption occurs the refractive index consists of an imaginary as well as a real part, $\eta = n + ik$. In an absorbing medium one can compute the complex refractive index η for a dielectric with bound electrons by considering the electrons as classical damped harmonic oscillators:

$$\eta^2 = (n + ik)^2 = 1 + \frac{Ne^2}{m\epsilon_0}\left(\frac{(\omega_0^2 - \omega^2) + i\gamma\omega}{(\omega_0^2 - \omega^2)^2 + \gamma^2\omega^2}\right) \qquad \text{II.7}$$

Where N = number of electrons per unit volume

e = electron charge

m = electron mass

ϵ_0 = electrical permitivity

γ = dampening constant, or bandwidth in units of frequency

ω = frequency

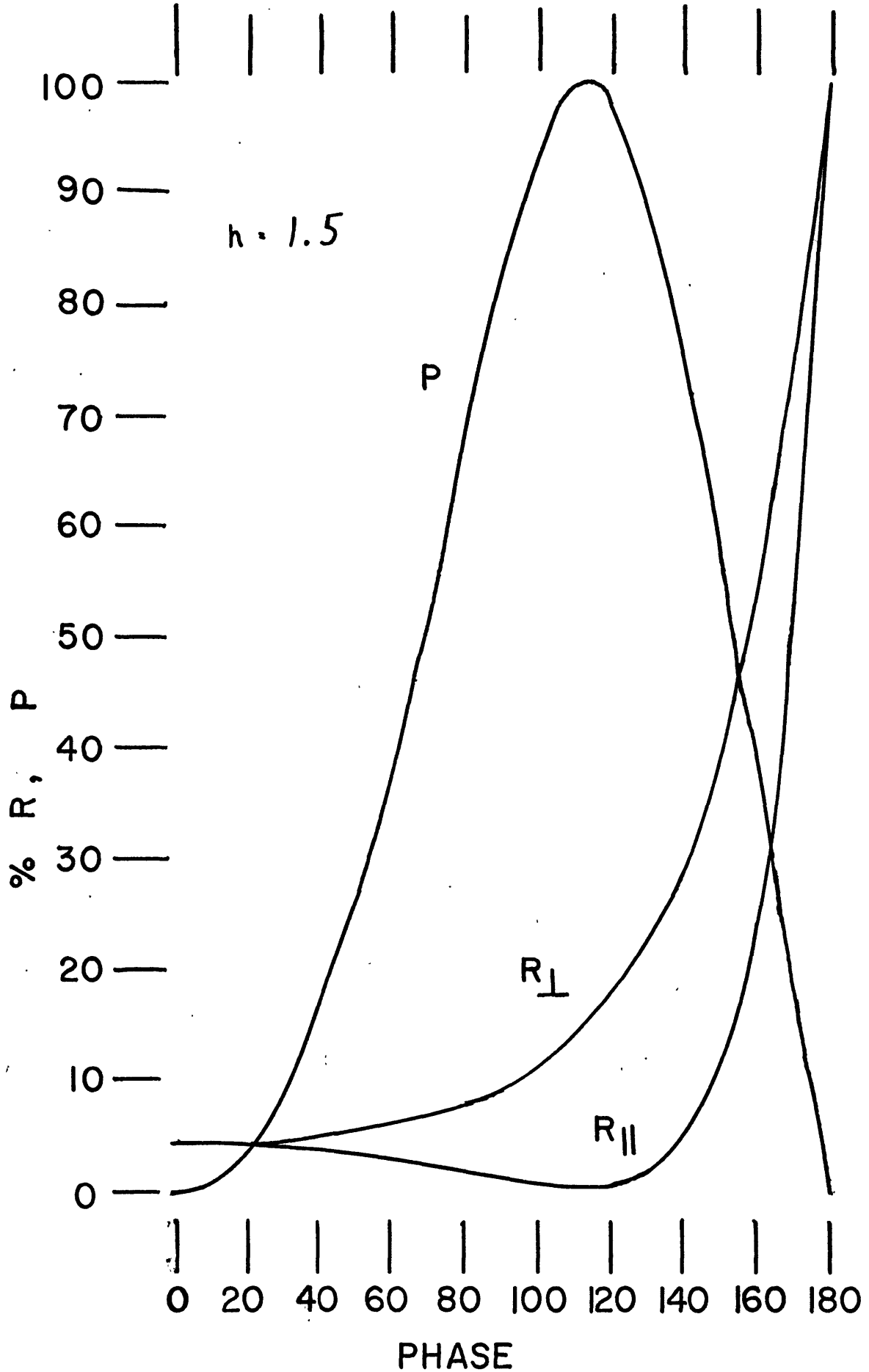

Figure II.1 Specular Reflection and Polarization for n = 1.5

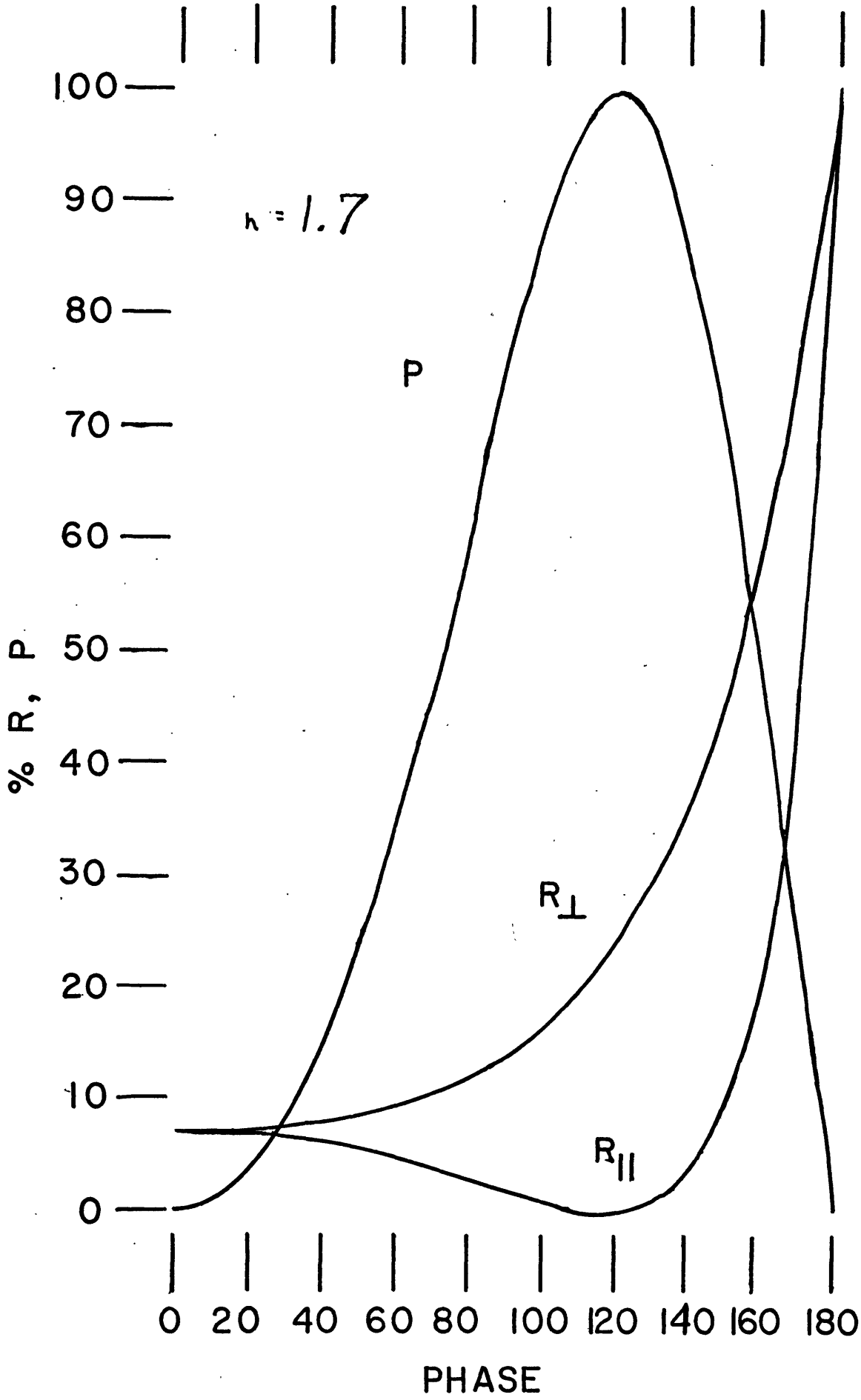

Figure II.2 Specular Reflection and Polarization for n = 1.7

ω_o = effective resonant frequency

n = real refractive index

k = extinction coefficent.

The above equation can be solved for n and k in terms of frequency by equating real and imaginary parts. Figure II.3 shows how these two quantities vary close to the resonant frequency.

Light transmitted through a given thickness of material, z, is attenuated exponentially by the coefficent of absorption a:

$$I = I_o e^{-az} \qquad \text{where } a = \frac{\omega}{c} k \qquad \text{II.8}$$

and c is the velocity of light.

Thus, the variation of k describes absorption bands.

If there are more than one resonant frequencies, a summation is necessary for $\eta(\omega)$:

$$\eta^2_{(\omega)} = 1 + \frac{Ne^2}{m \epsilon_o} \sum_j \frac{f_j \left[(\omega_{o_j}^2 - \omega^2) + i \gamma_j \omega \right]}{(\omega_{o_j}^2 - \omega^2)^2 + \gamma_j^2 \omega^2} \qquad \text{II.9}$$

where f_j are the fractional oscillator strengths. For a solid, f_j and γ_j of an atom are affected by the surrounding atoms.

In section III these equations will be tailored to describe a crystal field absorption, and reflection from a particulate surface of such a substance will be modeled within limits.

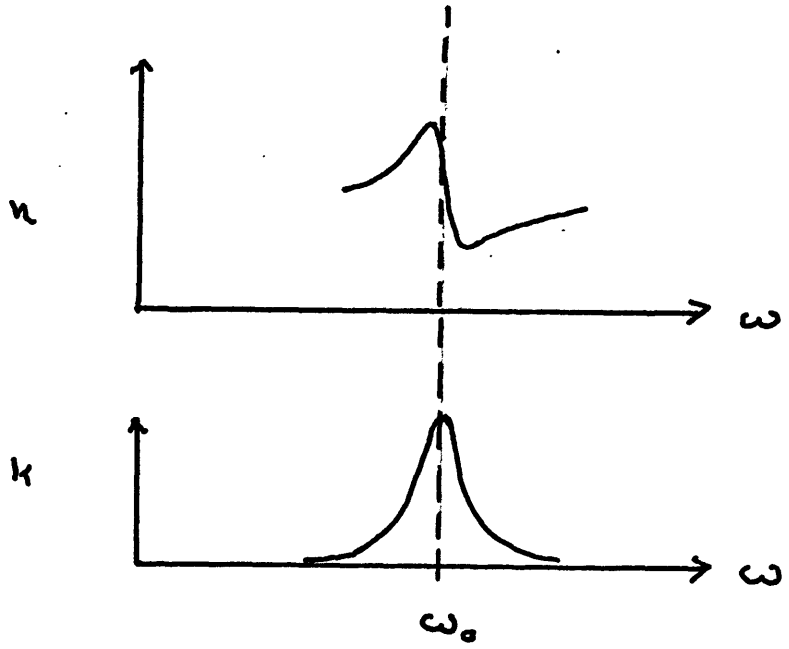

Figure II.3 Real Refractive Index n and Extinction Coefficent k vs frequency in the region of an absorption band (from Fowles)

C. Reflection of Light from a Particulate Surface

Components of Reflection

Rock forming silicate minerals are dielectric solids, and reflection from such surfaces is described by Fresnel's equations. When light is incident on a particulate surface, a portion of it is specularly reflected from the first surface it meets, and a portion is transmitted through the particle (if it is non-opaque). The transmitted component encounters more boundaries and is reflected by and transmitted through numerous particles before it either is absorbed altogether or reaches the surface again and is propagated outward as diffuse light.

The mean optical path length (MOPL), or average distance traveled through the material, of this diffuse component is a function of both the average number of boundary reflections necessary to get incident light out again (which is controlled somewhat by porosity or compaction), and the distance traveled through the material between boundaries (controlled by particle size). The MOPL of the actual measured reflectivity is further complicated by the nonconstant ratio of the diffuse and specular components. For porous surfaces (most everything) these components do not vary in a simple relation to Fresnel's results. For increasing phase some of the first surface specular component is blocked by other particles and becomes part of the diffuse component. Thus, the total MOPL of a measured reflection is an intricate function of particle size,

porosity, and phase.

Compositional Information

Fortunately, much compositional information can be obtained from a reflection spectrum without knowing the MOPL. Reflectivity measurements will contain compositional information as long as there is a diffuse component (preferably large) of the reflected light that has passed through the particles of the surface. Unless saturation (near complete absorption) occurs, the wavelength and shape of absorption features, which are diagnostic of composition, do not depend on the MOPL; the magnitude of the absorption does. A mineral may be tentatively identified in a reflection spectrum, but the quantity is less clearly defined.

An important application of using reflectivity measurements to infer compositional information about a surface has been the telescopic and coordinated laboratory studies of lunar surface material. Of these studies, the one most relevant to the present discussion is described in the recent report by Adams and McCord (1972). It was shown that the wavelength of the absorption bands of pyroxenes varies in a regular, well defined way with the composition of the pyroxene. Absorption bands of returned lunar material not only correlate well with telescopically measured reflectivity of the sampling area, but they also correctly identify the composition of the absorbing pyroxene. The band position of the absorption is critical in compositional identification.

Polarization Information

The fact that a specular component remains in the reflection from a particulate surface is well demonstrated by the polarimetric studies by Dollfus, Gehrels, Pellicori, and others. The polarization vs phase of a particulate surface closely parallels that predicted by Fresnel's equations for a plane boundary except in magnitude. For a particulate surface, reflection is diluted by the diffuse component. For absorbing or opaque materials a small negative value of polarization occurs for phase angles less than about 25°. The magnitude of the maximum polarization generally varies inversely with the brightness of the substance: brighter substances have a larger diffuse component.

Figure II.4 illustrates the polarization of moonlight obtained by Pellicori in 1966-67 for two filters. Gehrels and Dollfus have both pointed out the wavelength dependence of polarization for the lunar surface. It seems to be again inversly correlated with the spectral reflectivity. This inverse relation is implied by the previous discussion of specular and diffuse components in the first section of II.C. An increase in the absorption of the diffuse component would not only decrease the total reflectivity, but would also cause an increase in the ratio of specular to diffuse reflection and thus an increase of polarization. This is the basis of the reasoning for the polarimetric sutdy presented in the following sections.

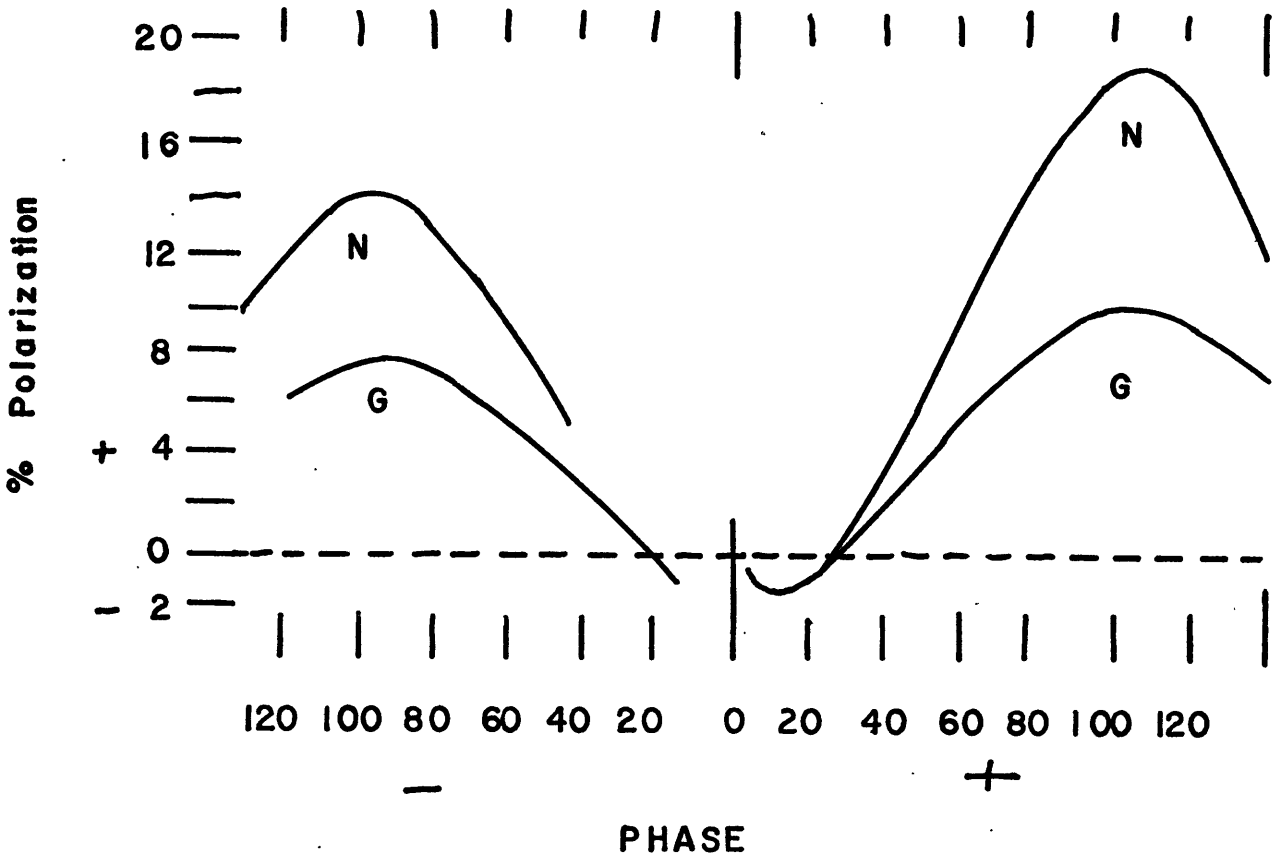

Figure II.4 Polarization vs phase (Pellicori 1969) for the moon. The wavelengths of the two filters are N = .336μ and G = .519μ .

III. Fresnel's Equations Applied To the Spectral Region of a Transition Metal Absorption Band

The variables and constants of Fresnel's equations were tailored to describe the spectral region around a crystal field absorption. A computer program was written to examine the implications of these equations. The first part of this section will discuss the tailoring; the next section will discuss the results.

A. Variables, Constants, and Equations

Complex Refractive Index

The actual form of equation II.9 used is:

$$\eta^2_{(\omega_k)} = (n + ik)^2 = (1.5)^2 + \frac{Ne^2}{m\epsilon_o} \sum_j \frac{F_j \left[(\omega_{oj}^2 - \omega_k^2) + i\gamma_k \omega_k\right]}{(\omega_{oj}^2 - \omega_k^2)^2 + \gamma_k^2 \omega_k^2} \qquad \text{III.1}$$

$$= A_k + iB_k \qquad \text{III.2}$$

where

$$\text{real } A_k = (1.5)^2 + \frac{Ne^2}{m\epsilon_o} \sum_j \frac{F_j (\omega_{oj}^2 - \omega_k^2)}{(\omega_{oj}^2 - \omega_k^2)^2 + \gamma_k^2 \omega_k^2} \qquad \text{III.3}$$

$$\text{complex } B_k = \frac{Ne^2}{m\epsilon_o} \sum_j \frac{F_j \gamma_k \omega_k}{(\omega_{oj}^2 - \omega_k^2)^2 + \gamma_k^2 \omega_k^2} \qquad \text{III.4}$$

and

$$n = \left[\tfrac{1}{2}(\sqrt{A^2 + B^2} + A)\right]^{\frac{1}{2}} \qquad \text{III.5}$$

$$k = \left[\tfrac{1}{2}(\sqrt{A^2 + B^2} - A)\right]^{\frac{1}{2}} \qquad \text{III.6}$$

η is calculated for 31 frequencies (ω_k) spaced 100Å apart from 0.8μ to 1.1μ. For each of these k frequencies the summation includes the contributions from 101 (j) nearby resonant absorption frequencies ω_{oj} spaced $\gamma_k/20$ apart.

Constants:

$e^2 = 2.5667 \times 10^{-37}$ coul^2

$m = 9.1091 \times 10^{-31}$ Kg

$\epsilon_o = 8.854 \times 10^{-12}$ farad/meter

$N = 10^{28}$ number/meter^3

Chosen Values:

$\omega_o = 1.98 \times 10^{15}$ sec^{-1}

$\gamma_k = \omega_k/Q$ dampening factor for each 'oscillator'

$F_j = C_2 e^{-C_3(\omega_o - \omega_{oj})^2}$ the oscillator strength factor which describes the gaussian distribution of resonant frequencies (ω_{oj}) centered on ω_o, which corresponds to a band centered at 0.95 microns.

$\Gamma = 2/\sqrt{C_3}$ the bandwidth of the gaussian distribution. In the program, the frequencies are converted to wavelength so that the bandwidth is 1000Å.

$C_3 = 0.04 \times 10^{-4}$

	case I	case II	
C_2 =	10^{-8}	10^{-9}	scaling factor of oscillator strength
Q =	10^2	10^3	related to γ as above.

The relationships between these factors is illustrated in figure III.1 which shows the contributions to the calculation of k.

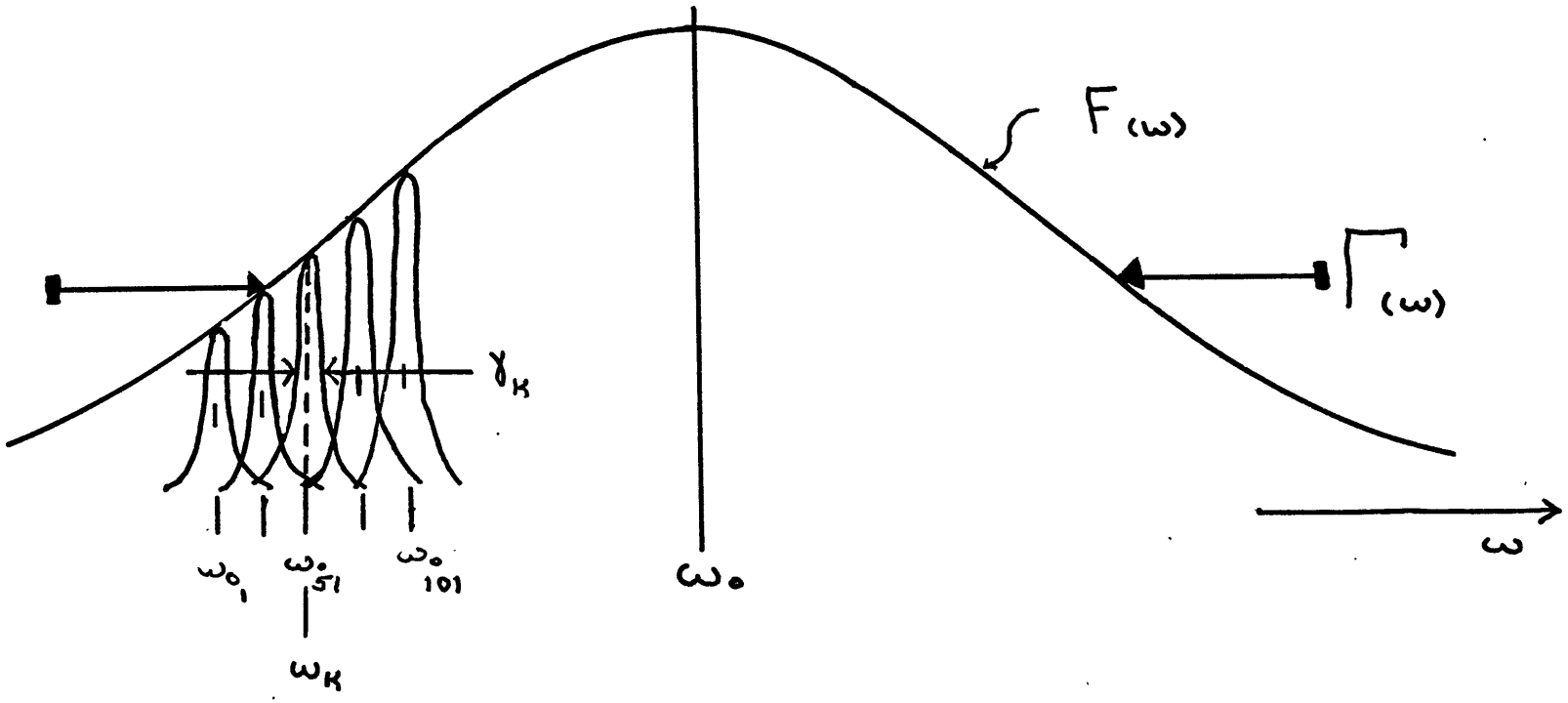

Figure III.1 Components of the Summation for the complex refractive index.

Empirical Requirements

An absorption band centered at 0.95 microns with a bandwidth of 1000Å is a reasonable, although narrow, description of an Fe^{+2} absorption in pyroxene. Ignoring the directional properties of the crystal, the gaussian distribution and summation of oscillator strengths is used to approximate the distribution of resonant frequencies due to lattice vibrations. For the observed absorption coefficents, k must be of the order of 10^{-3} to 10^{-4}.

The two values less clearly defined are 1) the 'normal' dampening constant γ_K (and thus Q) without lattice vibrations, and 2) the magnitude of the oscillator strength, which is one to two orders of magnitude less than C_2 (due to the summation). The combination of C_2 and Q in the equations must produce the required value of k.

Garbuny describes crystal field spectra for the lanthanides, which have f-f orbital transitions, with low oscillator strengths (10^{-6} to 10^{-5}) and high Q values ($\approx 10^4$). These values are not necessarily proper for the transition metals since the d electrons are more affected by the environment (less shielded by outer electrons) than are the f electrons of the lanthanides.

The two combinations of values for Q and C_2 were chosen for examination such that: I) $\gamma \leq \Gamma$ and II) $\gamma \ll \Gamma$. In case I $\gamma \approx 95$Å, or about $1/10\,\Gamma$; in case II $\gamma \approx 9.5$Å or about $1/100\,\Gamma$.

Once $\eta_{(\lambda)}$ was calculated for 31 wavelengths, Fresnel's

equations for reflection and transmission were used directly for phases 0° to 180° in intervals of 5°.

B. Results

Complex Refractive Index

There is a major difference in the two cases of γ described in the previous section for the real part of the complex refractive index. When γ of a single absorption is not greatly different from the halfwidth Γ of the lattice vibration distribution (case I), the dispersion character of n described in section II.B is also evident in the summation. However, when γ is much smaller than Γ (case II), the dispersion character is lost and n varies in a manner similiar to k. These cases are illustrated in figures III.2 and III.3.

The reason for the loss of dispersion can be found by examining the equations III.3,4 and 5. When $\omega_{oj} = \omega_k$, n is close to, but slightly greater than, 1.5. If γ is small the dispersions of individual oscillations are almost equal and tend to cancel in the summation. When γ is large cancellation is not complete. It would be difficult to tell which of these cases is more like the real case since the variation of n given by the equations is very small. For stronger absorptions of a different nature, the same effect of γ would be true except the variation of n is larger and can be measured. The spectra reported by Garbuny for quartz in the infrared show dispersion.

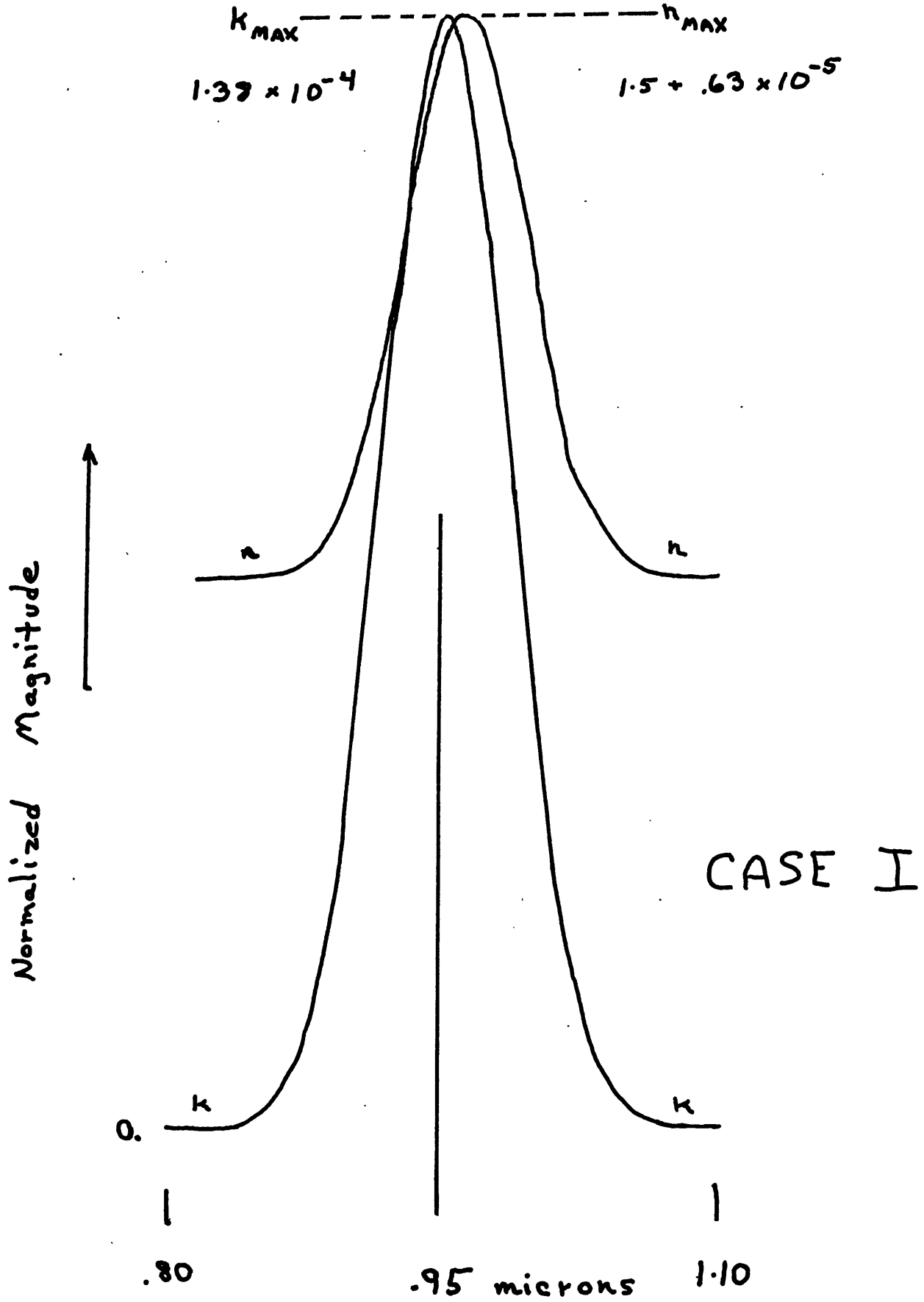

Figure III.2 Normalized values of $\bar{n}$ and $\bar{k}$ for Case I calculations of the complex refractive index.

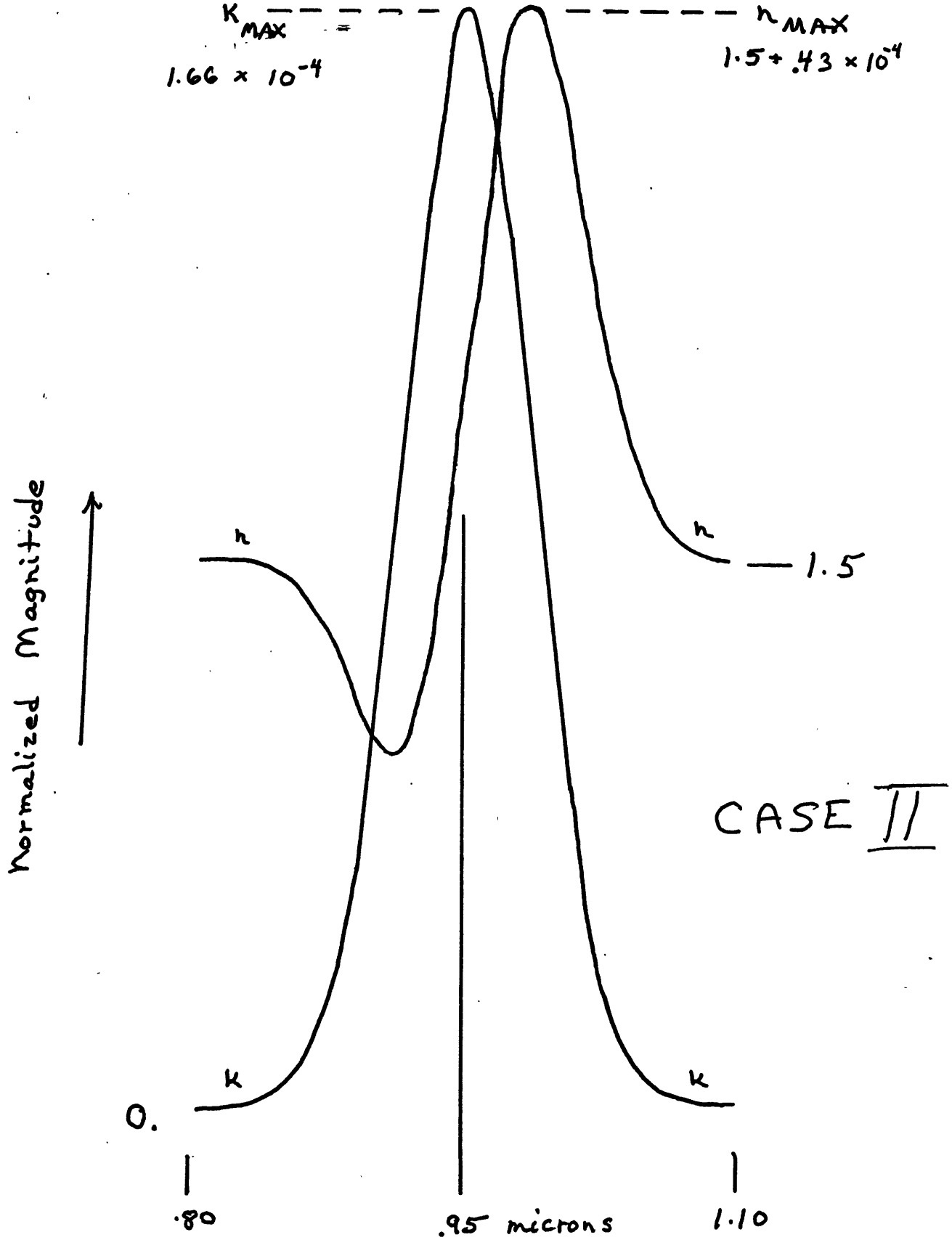

Figure III.3 Normalized values for n and k for Case II calculations of the complex refractive index.

Specular Reflection

Specular reflection is a function of η in Fresnel's equations. For strong absorptions, and thus large variations in k and n, the specular reflectivity was shown by computer calculations to vary in a manner similiar to the variation in n. For the transition metal ion absorption of a silicate discussed here, however, the variations of n and k are very small. The specular reflectivity is almost unaffected in the spectral region of such an absorption band and is essentially the same as that described by the equations for a real refractive index alone.

C. Models for Observed Reflectivity from a Particulate Surface

To model the observed reflectivity from Fresnel's equations one must decide:

1) the portion of specular component for each phase
2) the portion of diffuse (transmitted depolarized) component for each phase
3) the variation of the MOPL of the diffuse component with phase.

The diffuse component of reflection from a particulate surface was produced in the program by first allowing Fresnel's transmitted components to pass through the material for a MOPL distance and then depolarizing the remnant. A constant mean optical path length of 1 millimeter was chosen as a reasonable estimate (see Appendix A). Two models were produced for simple combinations of diffuse and specular components.

Model 1

Components are combined as they occur. The reflection from a particulate surface Rp is expressed for each wavelength as:

$$Rp_{\parallel} = R_{\parallel} + D$$

$$Rp_{\perp} = R_{\perp} + D$$

where $D = \frac{1}{2}(T_{\parallel} + T_{\perp}) \times e^{-a(MOPL)}$

and R and T are the specular reflection and transmission computed from Fresnel's equations, and a is the coefficent of absorption.

The effect of the above combination is to normalize the total reflectivity Rp_t to 100% outside the absorption

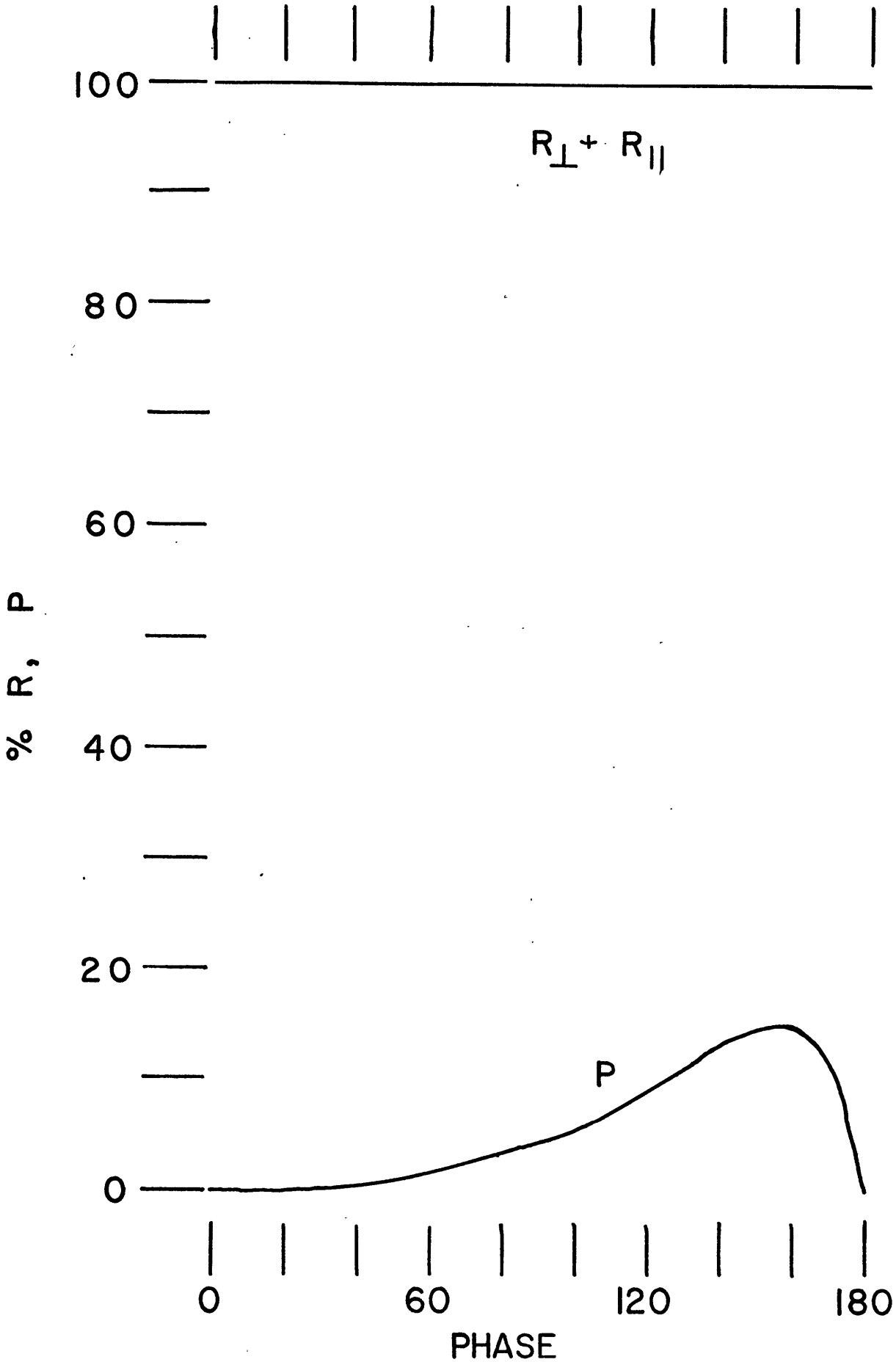

Figure III.4 Model 1: Reflectivity and Polarization at $\lambda = .80\mu$.

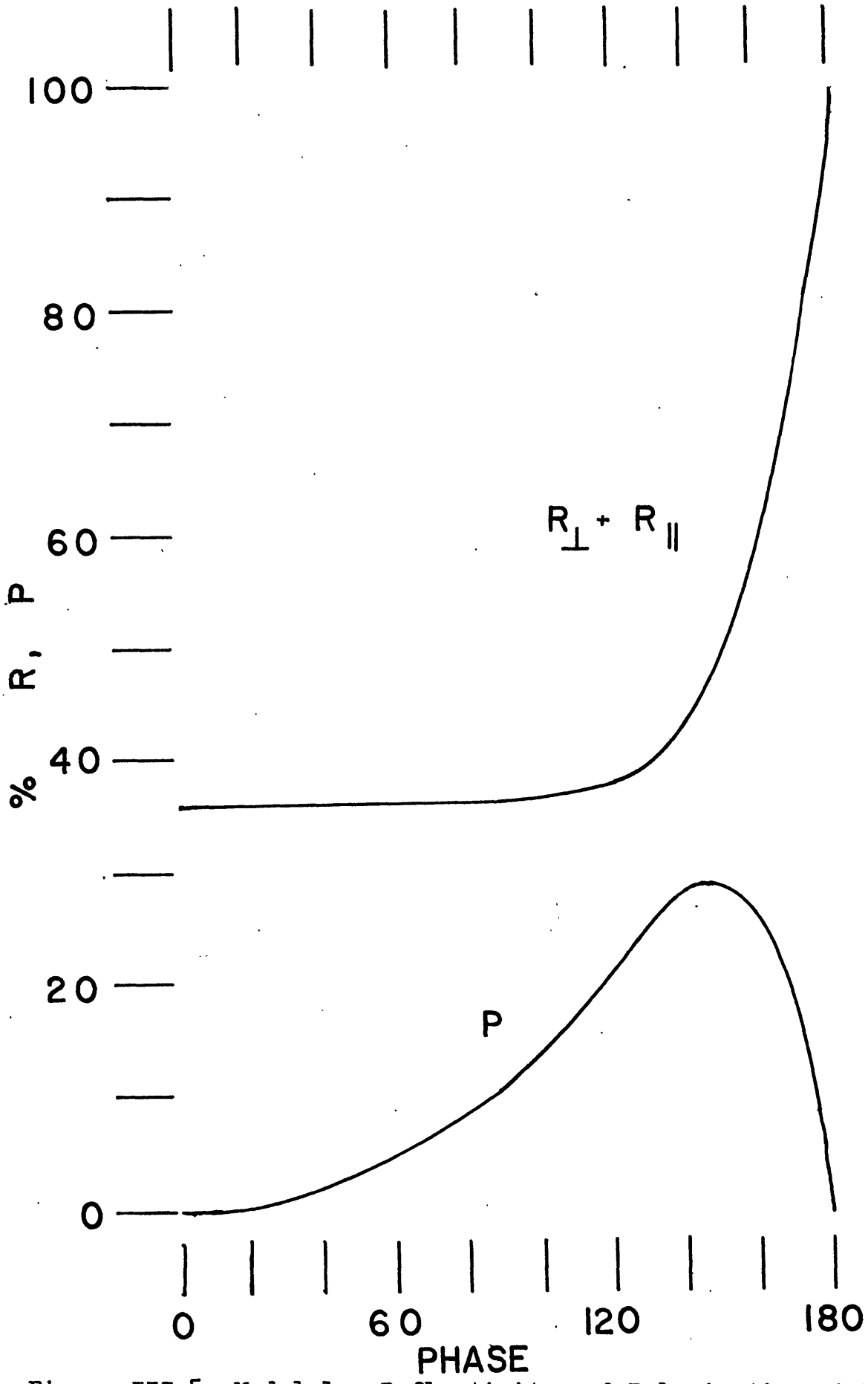

Figure III.5 Model 1: Reflectivity and Polarization at $\lambda = .95\mu$.

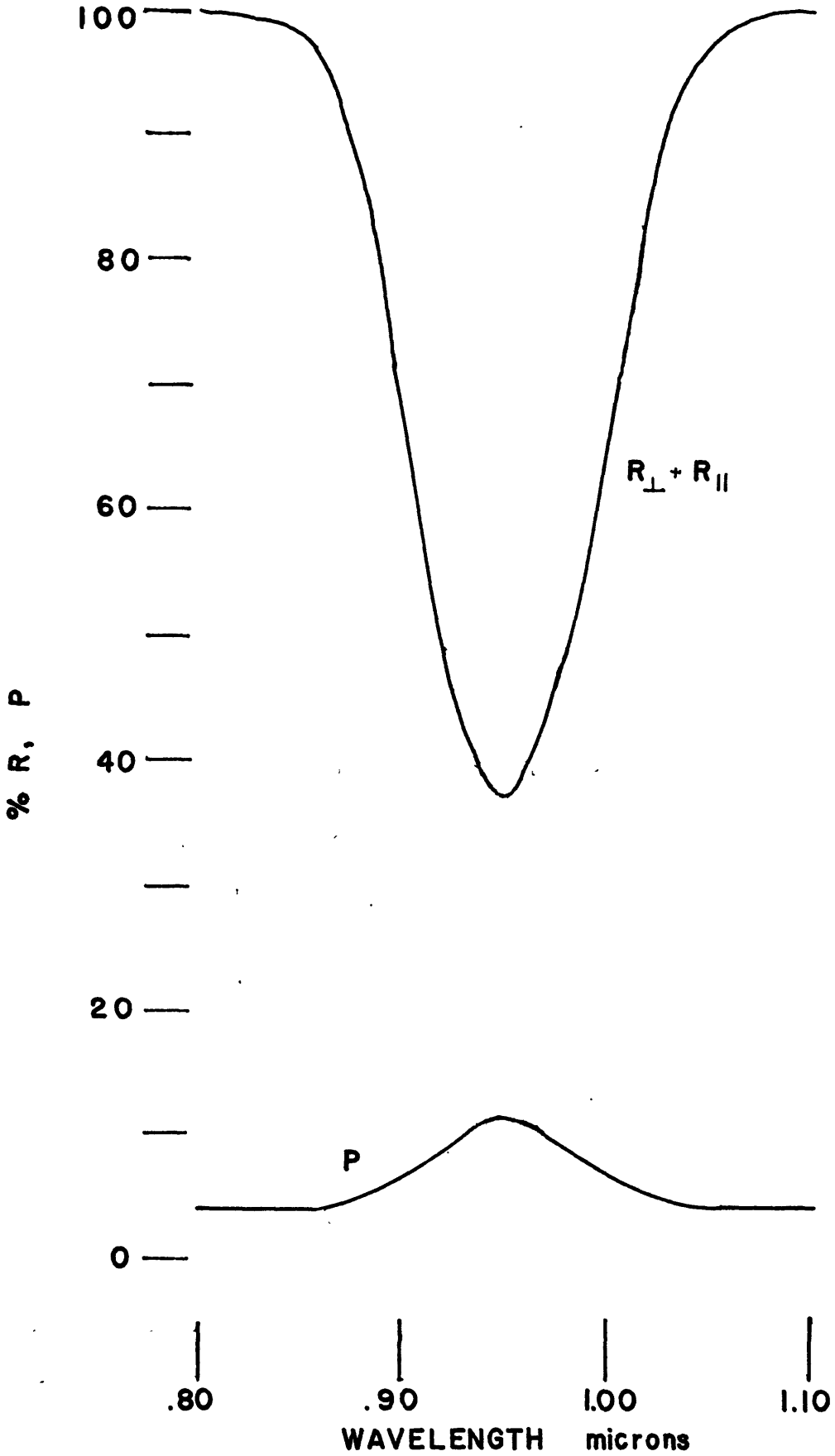

Figure III.6 Model 1: Reflectivity and Polarization at $\alpha = 90°$.

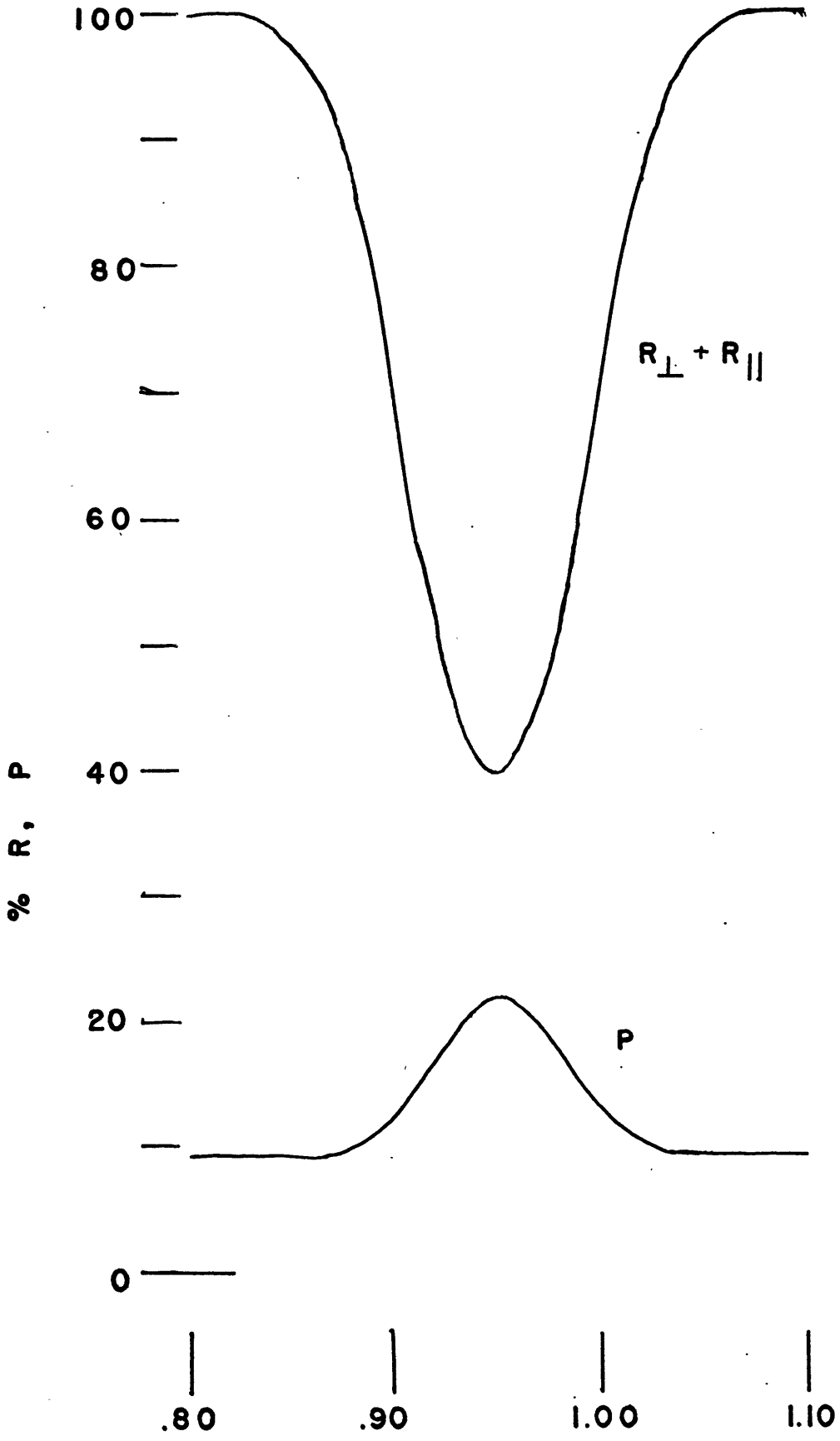

Figure III.7 Model 1: Reflectivity and Polarization at $\alpha = 120°$

band. Figures III.3 and III.4 show Rp_t and the corresponding polarization with phase for .80 micron and .95 micron respectively. Figures III.5 and III.6 show Rp_t and the corresponding polarization vs wavelength for a phase of 90° and 120° respectively.

Model 2

Since the lunar surface has a maximum polarization of approximately 10%, the specular and diffuse components of the second model are combined to ensure a ratio of 1 : 9 outside the absorption band for each phase.

$$Rp_{\parallel} = R_{\parallel} \times \frac{.10}{X} + .90D$$

$$Rp_{\perp} = R_{\perp} \times \frac{.10}{X} + .90D$$

where $X = \frac{R_{\parallel} + R_{\perp}}{2D}$ at .80 microns and the other variables are as in the previous model.

This procedure normalizes the reflectivity to 96% at .80 microns and zero phase. Figures III.7 and III.8 show Rp_t and the corresponding polarization with phase for .80 and .95 microns respectively. Figures III.9 and III.10 show Rp_t and the corresponding polarization vs wavelength for a phase of 90° and 120° respectively.

Discussion

Although neither model is correct for all phases, they do provide two pieces of useful information. I.) An examination of the phase for the maximum polarization, P_{max},

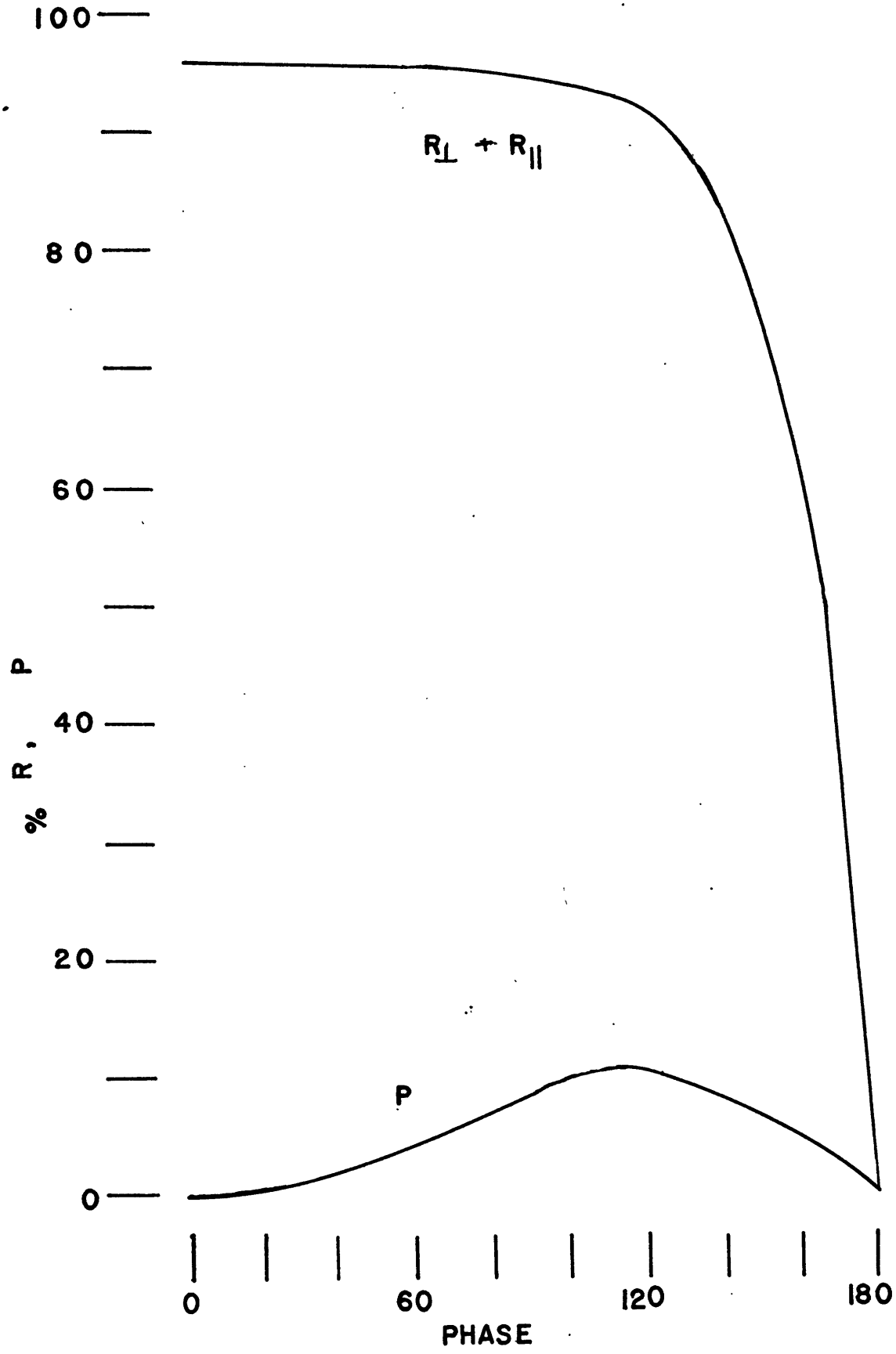

Figure III.8 Model 2: Reflectivity and Polarization at $\lambda = .80\mu$

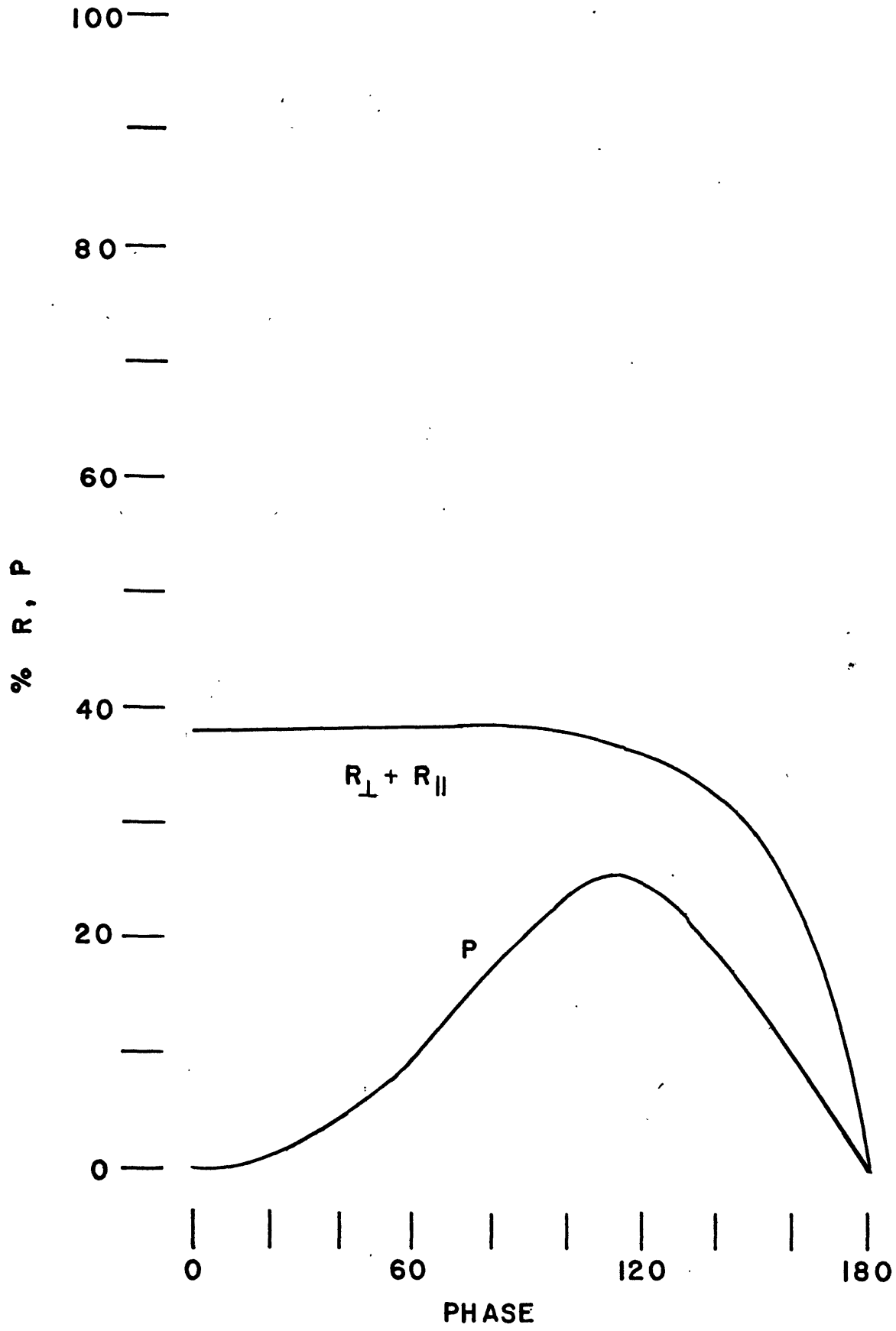

Figure III.9 Model 2: Reflectivity and Polarization at $\lambda = .95\mu$.

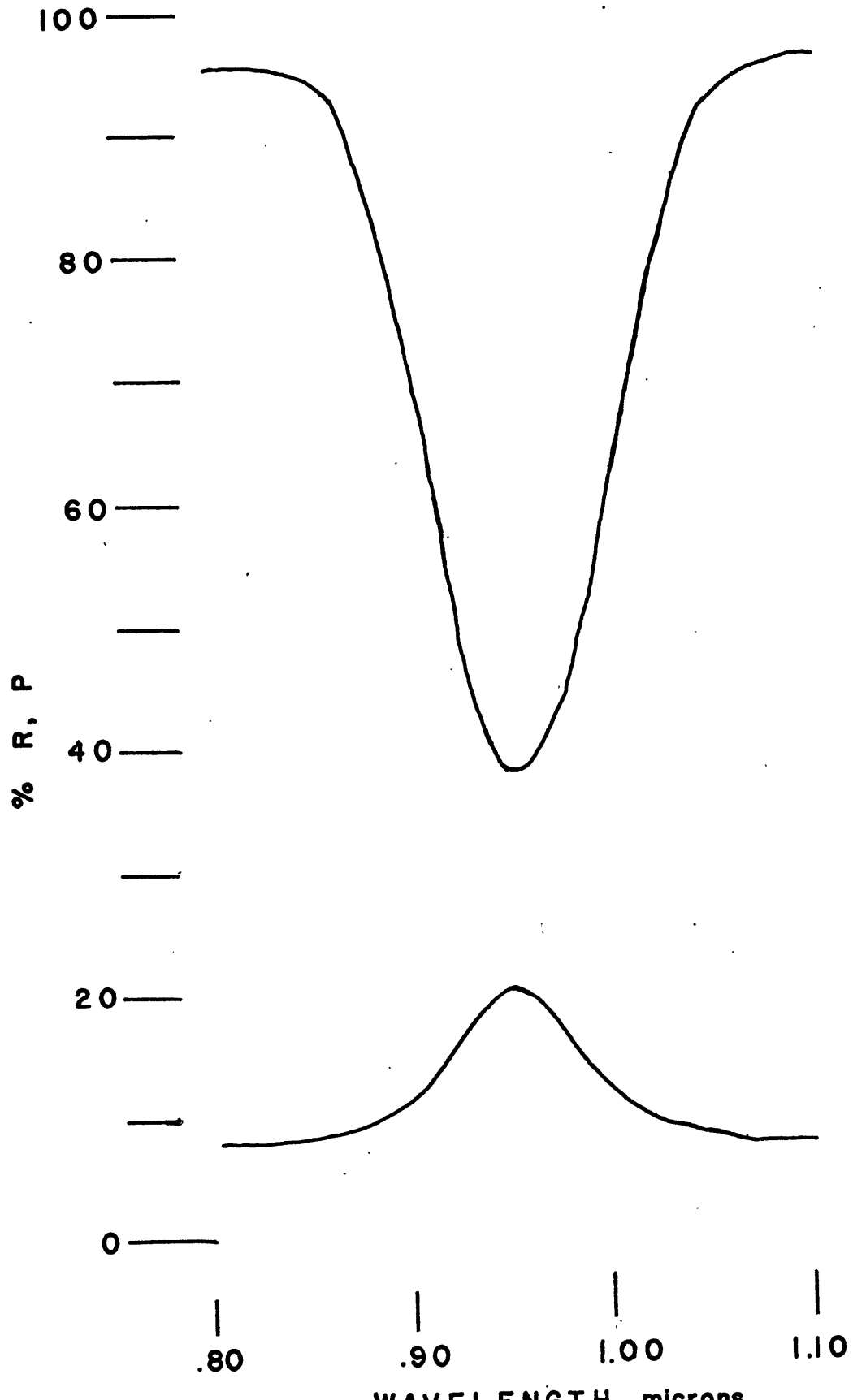

Figure III.10 Model 2: Reflectivity and Polarization at $\alpha = 90°$

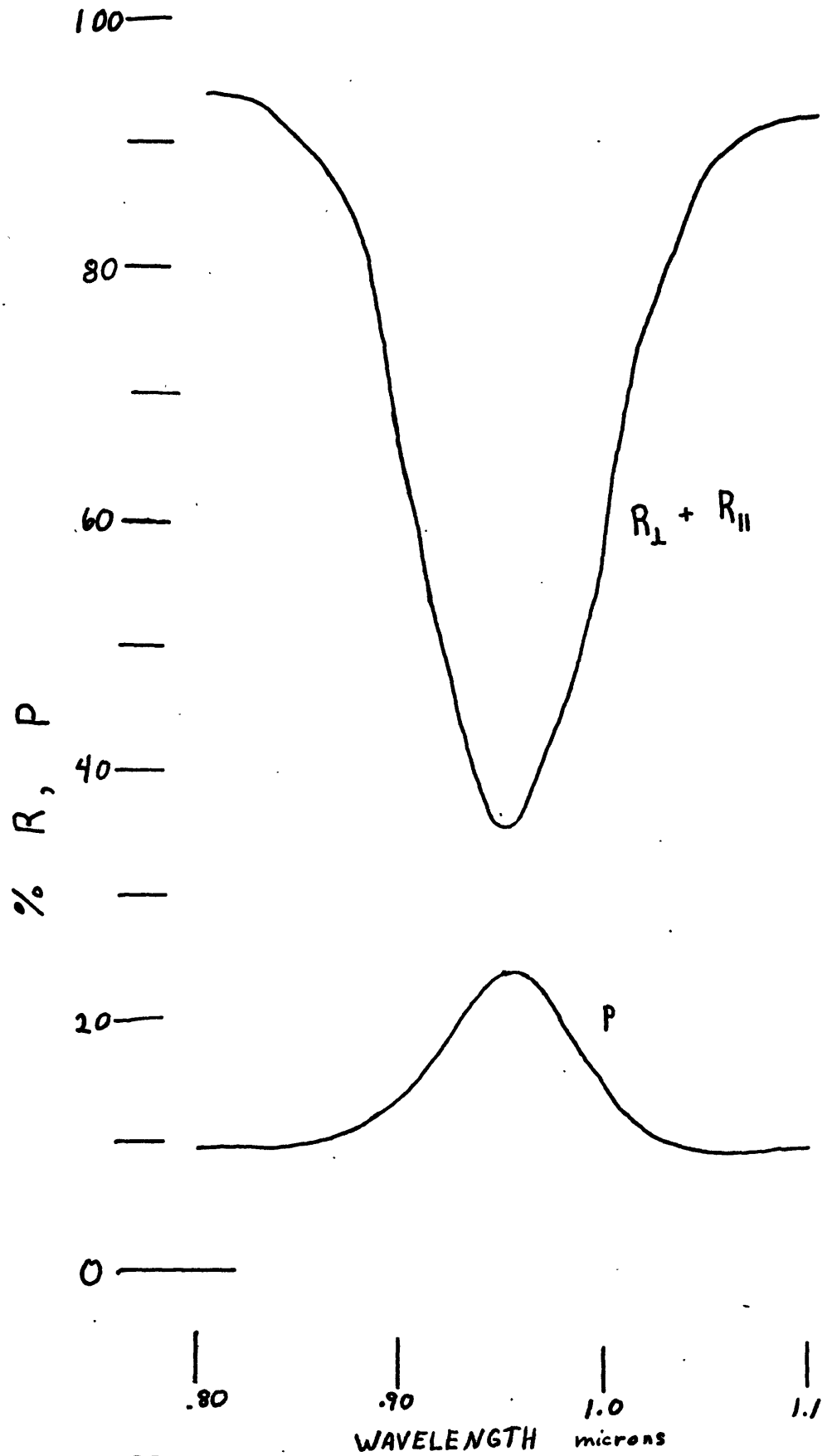

Figure III.11 Model 2; Reflectivity and Polarization at $\alpha = 120°$

for both models indicates that the phase of P_{max} is clearly a function of the mixture of components and not simply an indicator of the real refractive index n. This easily explains the failure of experimentalists to be able to identify n of common minerals by measurements of P_{max} using Brewster angle considerations for particulate surfaces. 2) Both models support the hypothesis set forth in the preface: at a phase when there is significant polarization of light reflected from a particulate surface, the amount of polarization increases in an absorption band.

A correct model for the lunar surface should be made to fit the following conditions:

1) The percent of the specular reflection remaining as a specular component would be highest at small phase and decrease rapidly as shadowing occurs. The portion of the specular component in the resultant reflectivity is complicated since the amount of specular reflection increases with phase.
2) The diffuse component would vary in a manner similiar to a lambert surface but would include parts of the specular component that have been blocked at high phase.
3) The combination of the two components would have to match the observed brightness vs phase for the moon.
4) The polarization of the total reflectivity would have to match that observed for the moon.

IV. Spectral and Polarimetric Analysis of Reflectivity in the Region of an Absorption Band

This section describes the laboratory measurements for well known samples. The study was undertaken to examine the reflectivity for various samples with an absorption band and to compare it to the variation of polarization in the same spectral region in order to determine the usefulness of spectral polarimetry as a diagnostic tool.

A. Description of Samples

The primary mineral chosen for the study is an orthopyroxene which is the dominent mineral of a Websterite. Earl Whipple of MIT handpicked a sample and with careful analysis found it to contain 6.04% iron of which 98.5% is Fe^{+2}. The sample is En_{89} in the enstatite-ferrosilite series $(Mg,Fe)_2Si_2O_6$.

A diffuse reflection spectrum of this sample made on a Cary 17 spectrometer is shown in figure IV.1. The Fe^{+2} spin allowed absorption band is centered at .91 microns. There is a second absorption band out of range in the infrared caused by further splitting of the d orbital energy levels of the Fe atom in a distorted octahedral site of the pyroxene. The enstatite may also contain some Al and perhaps Cr. The band position of the sample would be affected by an amount of Al in the pyroxene structure which would slightly alter the site symmetry. Further detailed chemical analysis is unavailable at the present. The small bands and spike

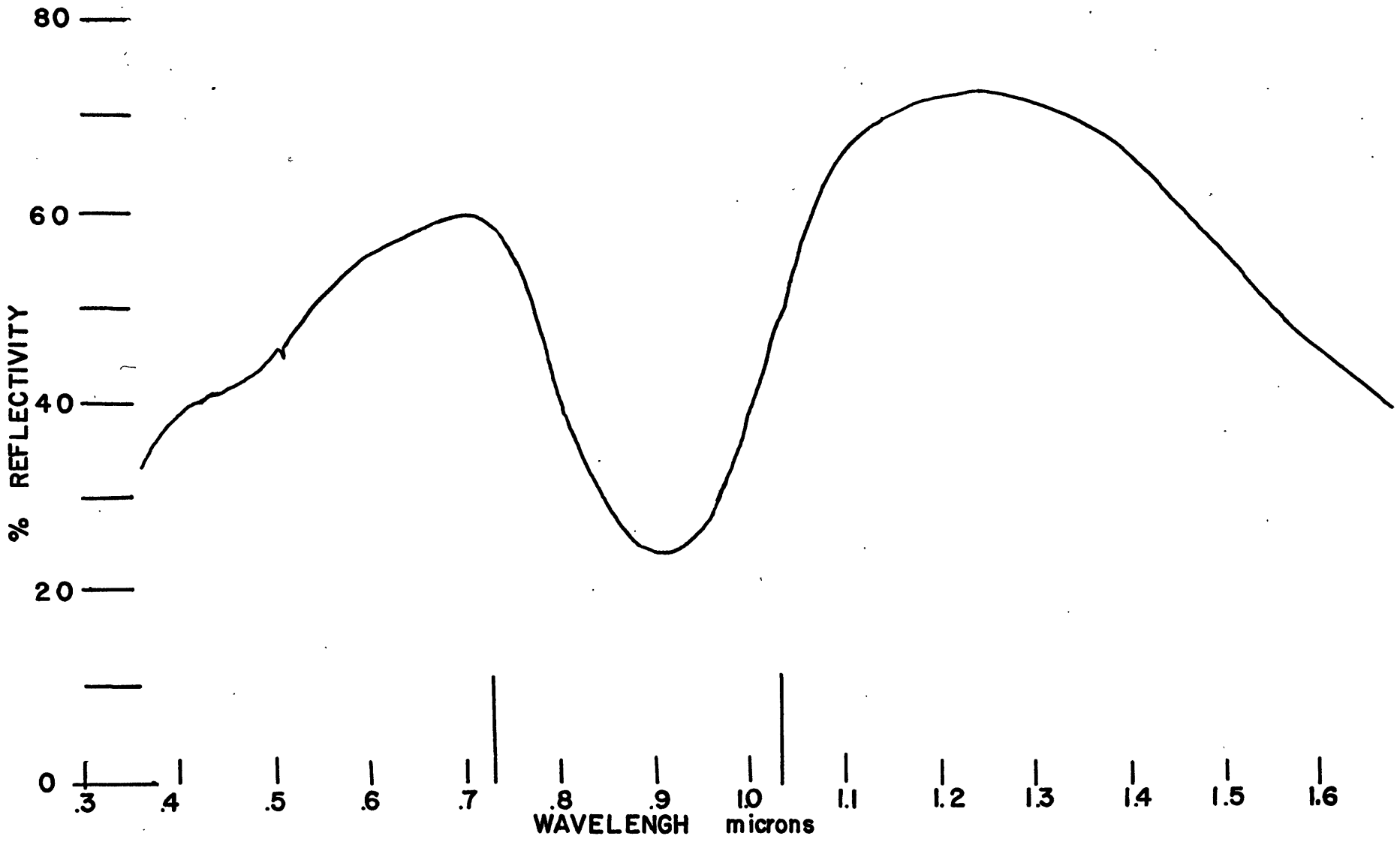

Figure IV.1 Diffuse Reflection Spectrum of Eu_{89}. The particle size is less than 125 microns.

around .4 and .5 microns are spin forbidden bands of Fe^{+2} and are therefore much less intense.

A larger sample of the same orthopyroxene was obtained from Jim Besancon of MIT to be used as the basis for the rest of the samples. It was found to be slightly contaminated (less than 1% of the total) with traces of a green clinopyroxene, an opaque, and hematite. The diffuse reflection spectrum is essentially identical with that shown in figure IV.1. None of the contaminants could be detected.

Table IV.1 lists the samples prepared for this study and the particle size. The samples with particle size $< 125\mu$ contain roughly equal amounts of $[125,63]\mu$ and $< 63\mu$. Those named E are 100% $enstatite_{89}$. Evf is a sample prepared by grinding part of E<63 for about 10 minutes. E100 and E<125 are the same sample. Those named Pxx contain xx% by volume plagioclase with the rest enstatite. The plagioclase is a hand picked oligoclase which is transparent in hand specimen. No traces of contaminants could be seen visually. Those named Mxx contain xx% magnetite by volume with the rest enstatite. The magnetite contains small amounts (less than 1%) of a red translucent regularly shaped mineral.

Table IV.1 Band depth of samples measured

1	2	3	4
		Rp(.91)/Rp(.73)	
SAMPLE	PARTICLE SIZE (microns)	DIFFUSE	90° phase
E [250,125]	250 > ps > 125	.29[1]	.25
E [125, 63]	125 > ps > 63	.29	.31
E<125	less than 125	.37	.38
E<63	less than 63	.47[2]	.44
Evf	very fine	.62[2]	.56
P100	less than 125	1.01	1.04
P90	less than 125	.74	.77
P50	less than 125	.50	.53
P10	less than 125	.37	.40
E100	less than 125	.37	.38
M10	less than 125	.49	.52
M50	less than 125	.74	.75
M90	less than 125	.87	.91
M100	less than 125	.87	.92

1 saturated band

2 partially packed

B. Diffuse Reflection Measurements

Diffuse reflection measurements were made on a Cary 17 spectrometer with a type II diffuse reflection attachment for all samples listed in Table IV.1. In this arrangement diffuse white light is incident on both a vertical sample and a smoked MgO standard. The light reflected in the normal position from both the sample and standard is analyzed by a monochrometer and detector. The measured reflectivity is the ratio of the reflectivity of the sample to that of the standard and is recorded on a chart recorder intricately calibrated with the Cary rates. The results presented here are transposed from longer data recordings and are shown in Figures IV.2, 3, and 4.

The values of reflectivity in figure IV.2 for different particle sizes demonstrate the principle 'the smaller the brighter' described by Adams and Filice. (1967). The apparent saturation that occurs in the the band for sample E [250,125] also occurs for unreported samples of larger particle sizes and indicates that the MOPL of the diffuse component for the large particles is so long that most of the light is absorbed. The light level recorded in the band comes from the specular component of reflection and part of the diffuse component with an optical path length less than the MOPL.

The effect of particle size on the total MOPL for these samples is best seen by measuring the band depth. The ratio of the intensity in the center of the band to that near the

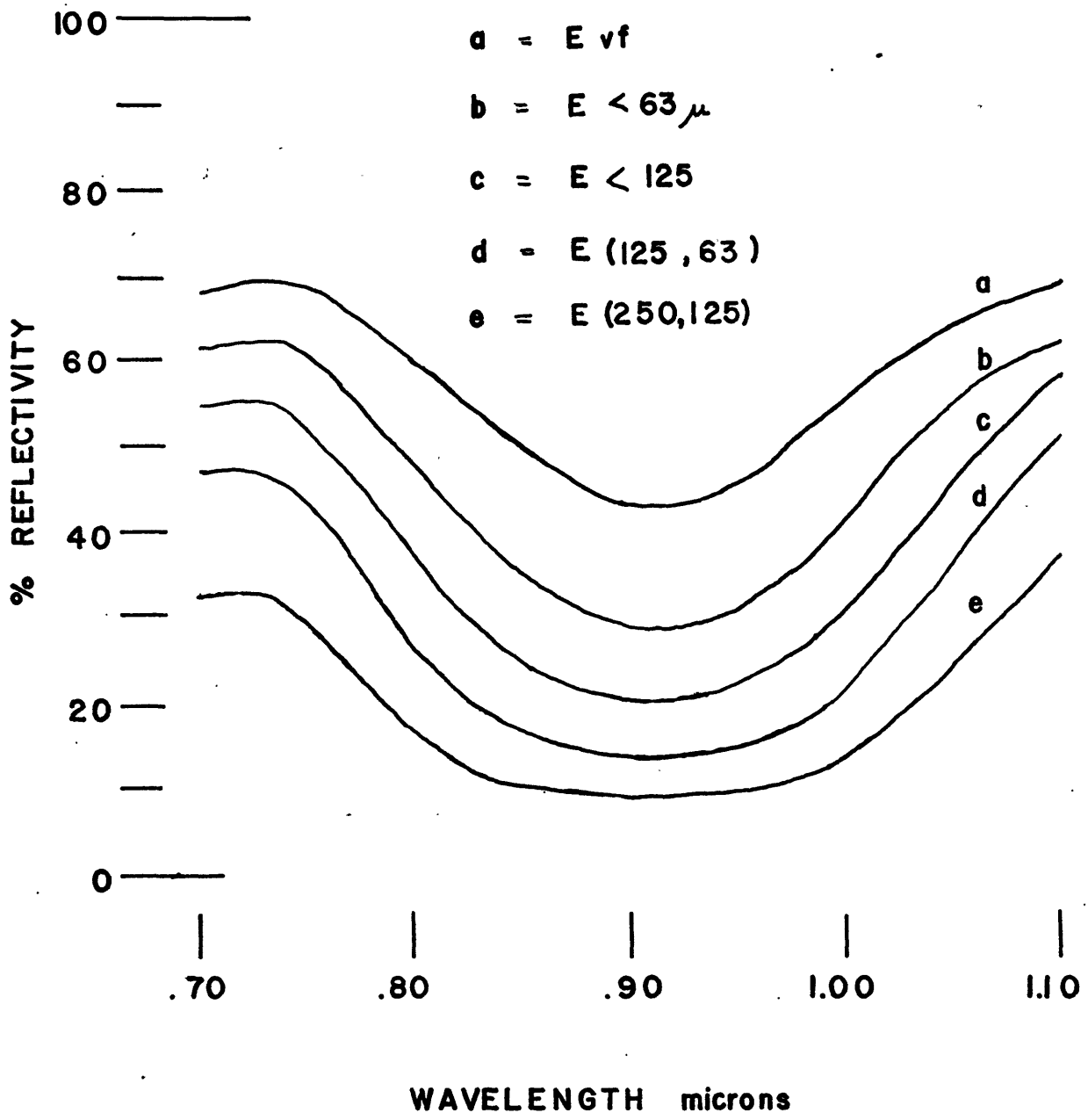

Figure IV.2 Diffuse Reflection Spectra of Enstatite: different particle size.

edge is listed in column 3 of Table IV.1. Except for the case of saturation, as the particle size decreases the band depth also decreases indicating a decrease in the total MOPL. For the smallest size samples, preparation for a vertical position measurement, which involves pouring into a sample dish and covering with a glass cover, causes the sample to become somewhat packed. Thus, for Evf and E<63 the MOPL is shorter than the other samples not only because the particles are smaller, but also because they are packed.

E<125 was chosen as the particle size for mixing with other minerals since it is similiar to particle sizes for lunar soil and has a MOPL that is fairly large but without saturation. The magnetite and plagioclase of Figures IV.3 and IV.4 have opposite effects on the mixtures. The opaque eats light, while the transparent mineral transmits it essentially without absorption, thus allowing a greater number of reflections and a greater probability of return to the surface.

The band depth ratios for the mixtures are also listed in table IV.1. For both types of mixtures the results indicate, as expected, that the mean optical path length through the enstatite decreases with dilution by another mineral. What is most striking is the effect of the <u>type</u> of mixture. The results indicate that only 10% opaques reduces the MOPL by an amount comparable to 50% dilution by a transparent mineral, and 50% opaques is comparable to 90% transparent mineral.

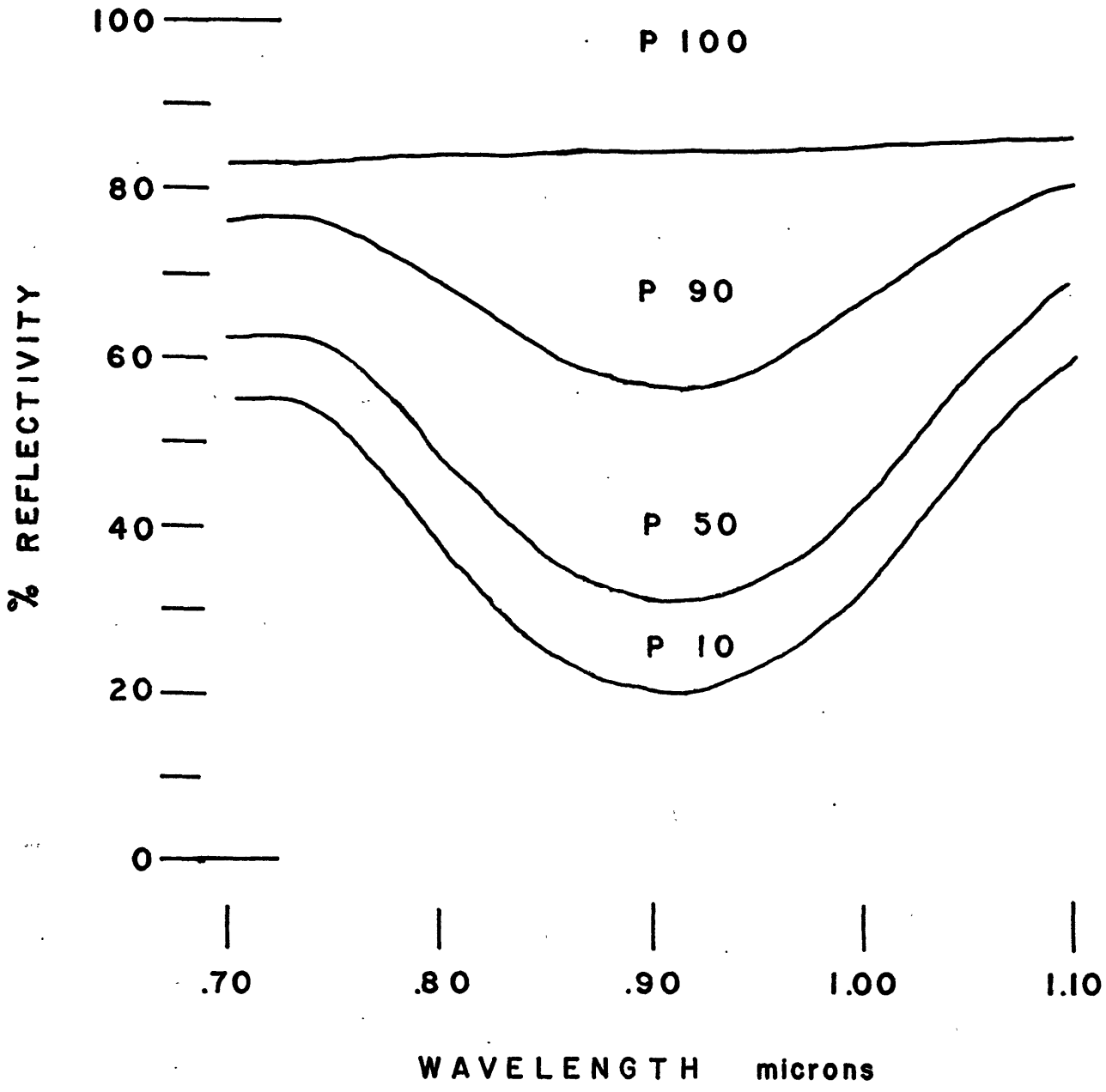

Figure IV.3 Diffuse Reflection Spectra of Enstatite: Plagioclase mixtures.

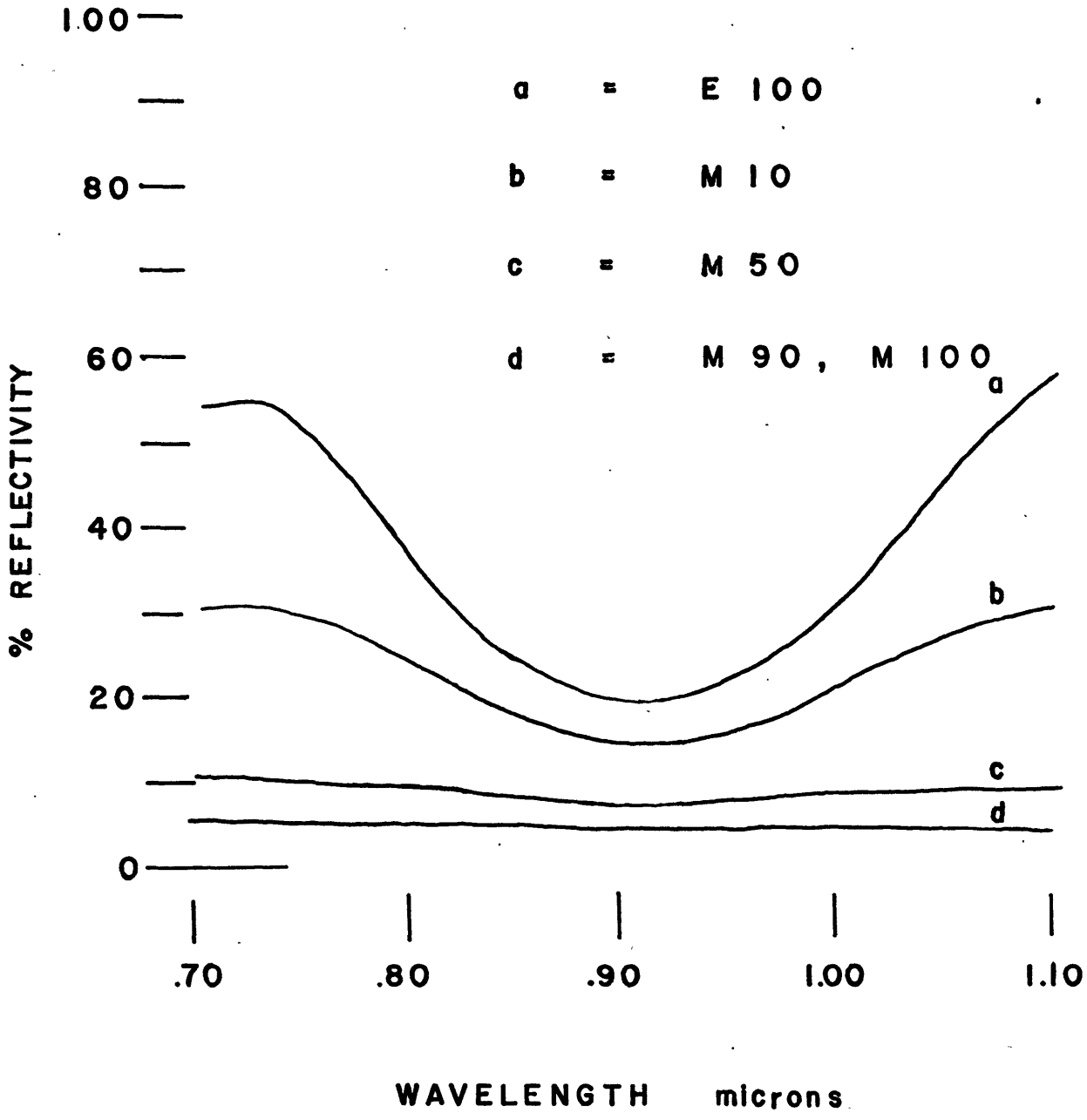

Figure IV.4 Diffuse Reflection Spectra of Enstatite: Magnetite mixtures.

C. Measurements at 90° Phase

Laboratory Techniques

Figure IV.5 shows schematically the laboratory arrangement for the measurements at 90° phase. A heath 701 series monochrometer and tungesten lamp were used to provide monochromatic light to 1.03 microns with a bandwidth of 40Å. The detector used for the measurements was an ITT FW-118 (s-1) photomultiplier cooled to dry ice temperatures. A pulse counting data system was used with a Fabritek instrument computer as the main unit and a Cipher magnetic tape recorder. This allowed most of the data handling to be done by computer. Combining the scan rate of the monochrometer, the integration time of the Fabritek, and the data process averaging, the effective sampling was every 20Å.

Prior to sample measurement two polaroids (HR) were calibrated. It was found that the crossed polaroids allow transmission of a maximum of only 0.2% of the light transmitted when the polaroids are oriented parallel to each other. The spectral range examined was from 6500Å to 12000Å. The polaroids themselves have a sharp cutoff below 7300Å, but their polarizing properties extend beyond 12000Å. The two polaroids were alligned so they could easily be fixed to either of two orthogonal positions: L position parallel to the plane of scattering (in the plane of the page for figure IV.5 A), and R position perpendicular to the plane of scattering. Each was also oriented so that its surface

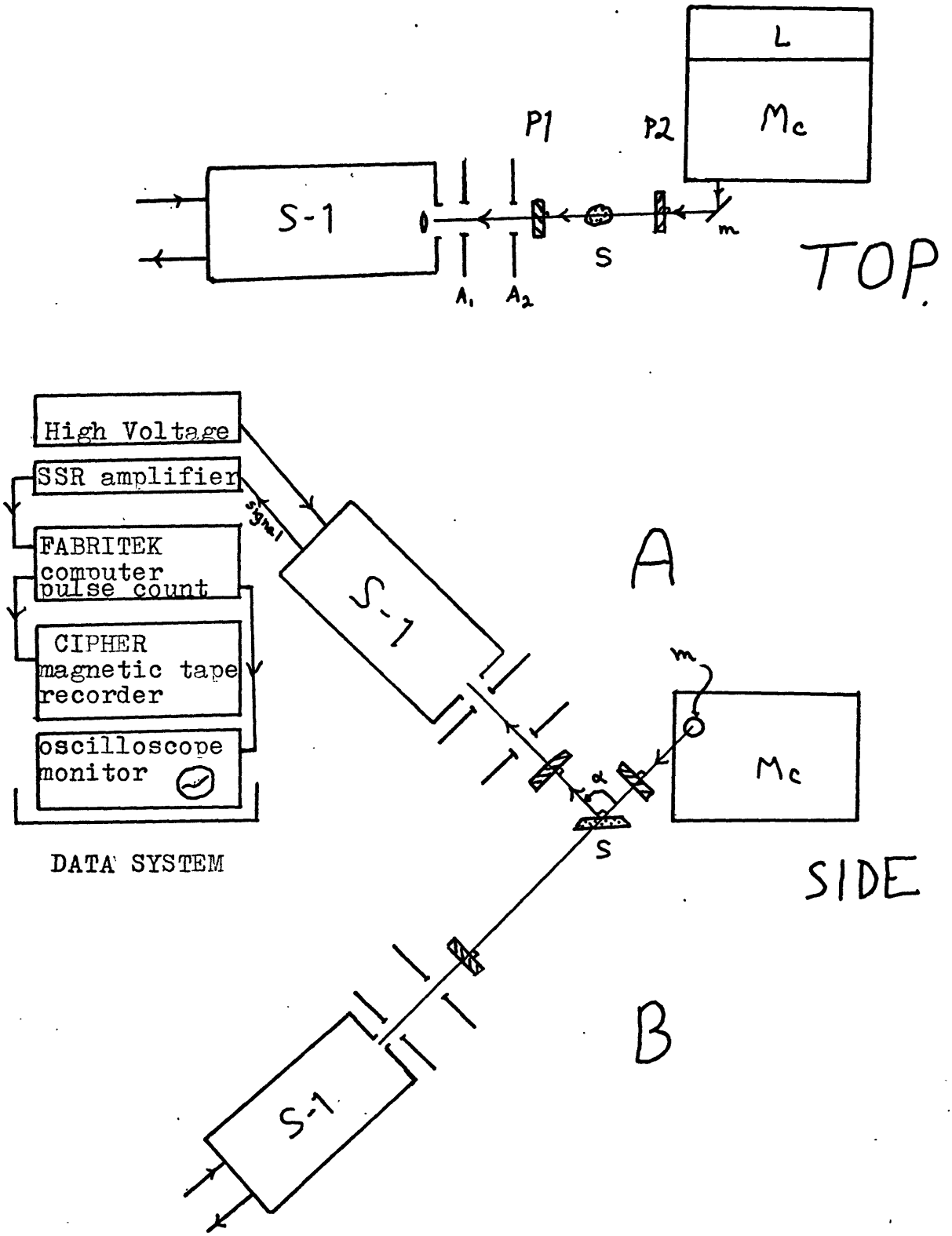

Figure IV.5 Schematic of the laboratory arrangement for measuring polarization. Position A is used to measure the four reflection components of the sample. Position B of the same equipment with the sample removed measures the two components of the source. $\alpha = 90°$, m = front surfaced mirror, P1,P2 = HR polaroids, S = sample, $A_1 A_2$ = two aperatures, S-1 = cooled photomultiplier detector.

was perpendicular to the direction of propagation of the light passing through it.

The source was found to be approximately 20% polarized in the L direction as measured from position B. Six measurements are therefore required for a valid polarization spectrum: two of the source and four for the sample. One needs to measure all components of the reflection, correct them for the polarization of the source, and put them back together to give the intensity in the plane of scattering, I_L, and the intensity perpendicular to it, I_R, for an unpolarized source. (Thank heavens the light incident on the moon is essentially unpolarized!) Refer to the equation sequence of figure IV.6 for the following description of how to accomplish the correction.

Examine separately what happens to the light in the two unequal planes of polarization from the source, S_L and S_R. In each case a certain amount is specularly reflected, C, maintaining the plane of polarization of the source, and the rest is diffusely reflected, D, with no polarization. If one analyzes each of these two reflections with a polaroid (Pl) one obtains the four measurable components listed A on the top right of figure IV.6. The total light reflected in the two planes of polarization, I_L and I_R, is shown in B. To correct for the unequal source components, one forms the correction factor N and applies it in the indicated manner to obtain corrected values for I'_L and I'_R. From these one can calculate

Figure IV.6 Sequence of equations to correct for a polarized light source.

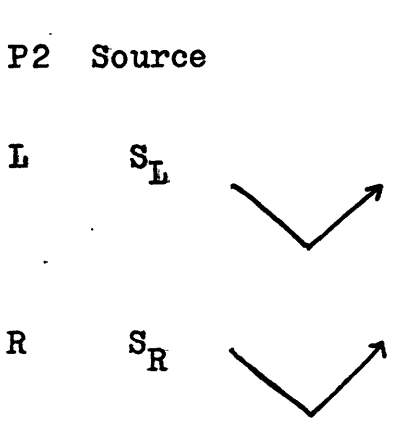

A

$$I_L = (C_L + \tfrac{1}{2}D_L)S_L + \tfrac{1}{2}D_R\ S_R$$

$$I_R = (C_R + \tfrac{1}{2}D_R)S_R + \tfrac{1}{2}D_L\ S_L$$

B

Correction factor $N = \dfrac{S_L}{S_R}$

$$I'_L = (C_L + \tfrac{1}{2}\ D_L)S_L + \tfrac{1}{2}D_R\ S_R \cdot N$$

$$I'_R = (C_R + \tfrac{1}{2}\ D_R)S_R \cdot N + \tfrac{1}{2}D_L\ S_L$$

C

Percent polarization $P = \dfrac{I'_R - I'_L}{I'_R + I'_L} \times 100$

the true polarization since the source cancels out as it should. This technique was used to obtain the polarization measurements reported here.

Smoked MgO was found to be polarized (see Appendix B) and absolute reflectivity measurements were prevented. For comparison with the diffuse reflectivity measurements of the previous section normalized reflectivity measurements were produced instead. Corrected measurements of the diffuse component reflection from MgO, D_{MgO}, was used as a standard. The normalized reflectivity scaled to unity at .73 microns is given as follows:

$$Rn(\lambda) = \frac{I'_L(\lambda) + I'_R(\lambda)}{D_{MgO}(\lambda)} \times \text{Norm}$$

$$\text{where Norm} = \frac{D_{MgO}(.73\mu)}{I'_L(.73\mu) + I'_R(.73\mu)} .$$

An important note concerns the texture of the samples. The sample was poured onto a flat surface. For all samples $< 125\mu$ this created a porous, hummocky (on the scale of millimeters) texture, which caused reflection to be relatively diffuse for bright samples.

Results

NORMALIZED REFLECTIVITY:

Normalized reflectivity measurements at 90° phase are shown in figures IV.7, 8, and 9. The error on the right of

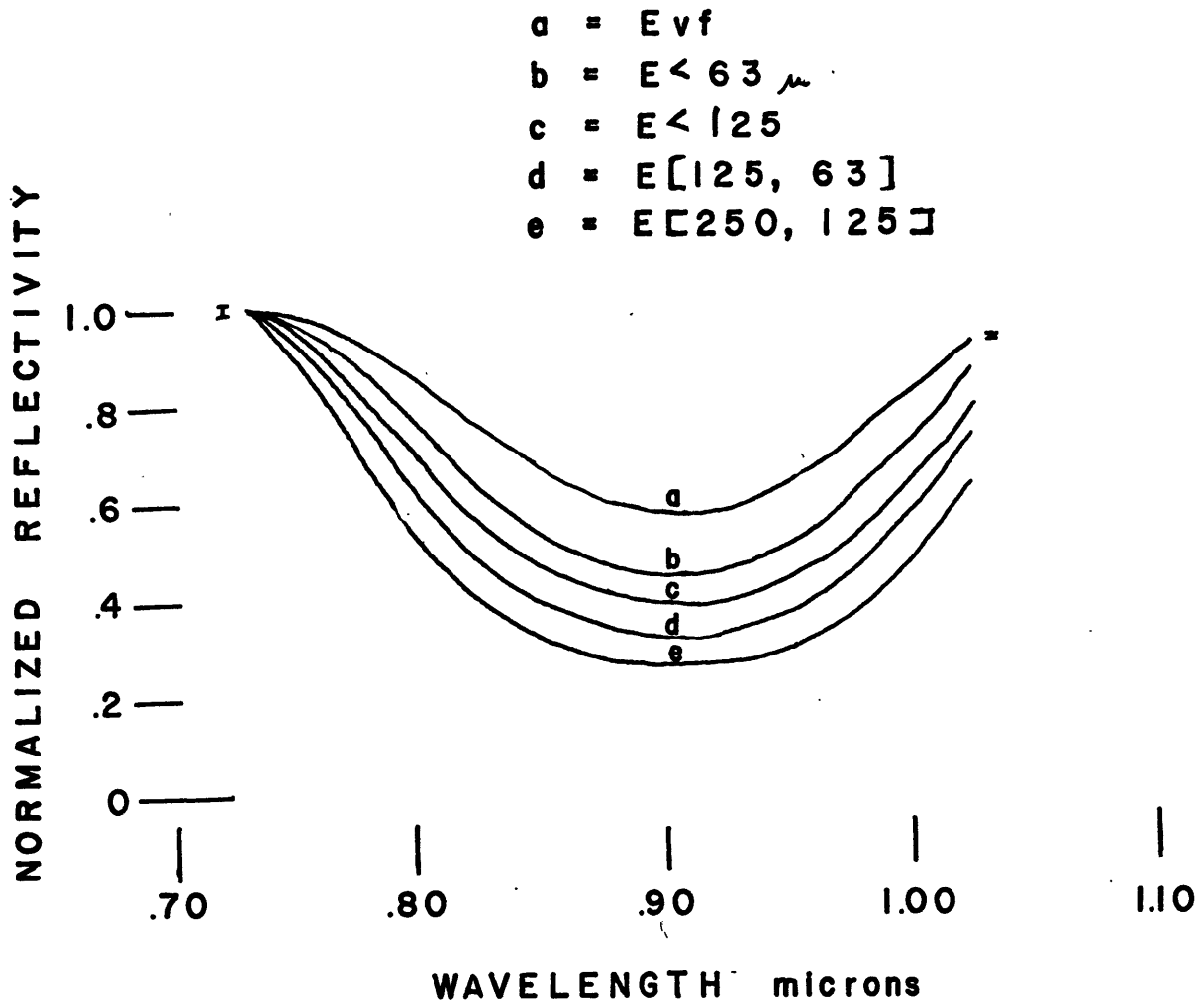

Figure IV. 7 Normalized Reflectivity of Enstatite: different particle size

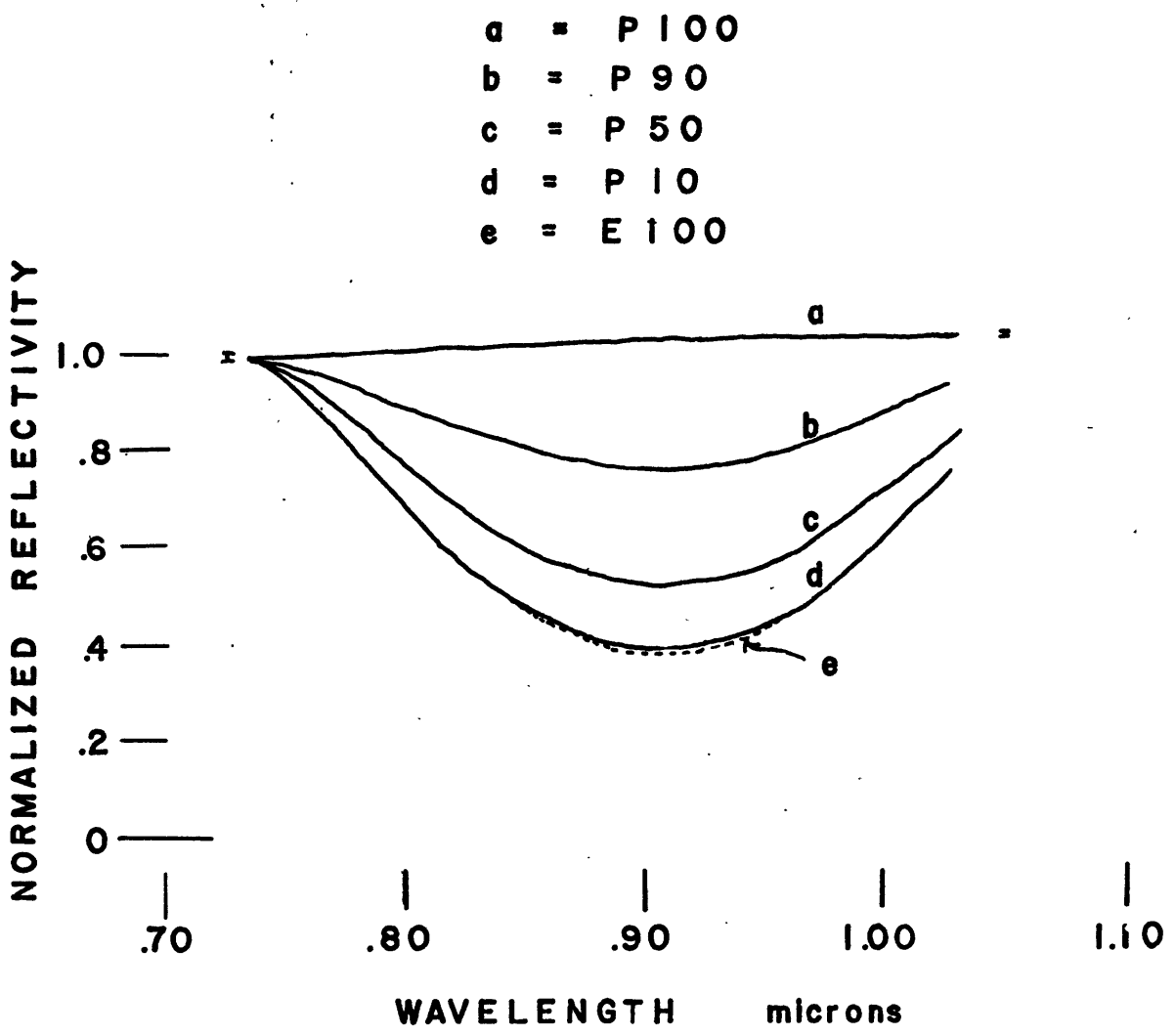

Figure IV.8 Normalized Reflectivity of Enstatite: Plagioclase mixtures.

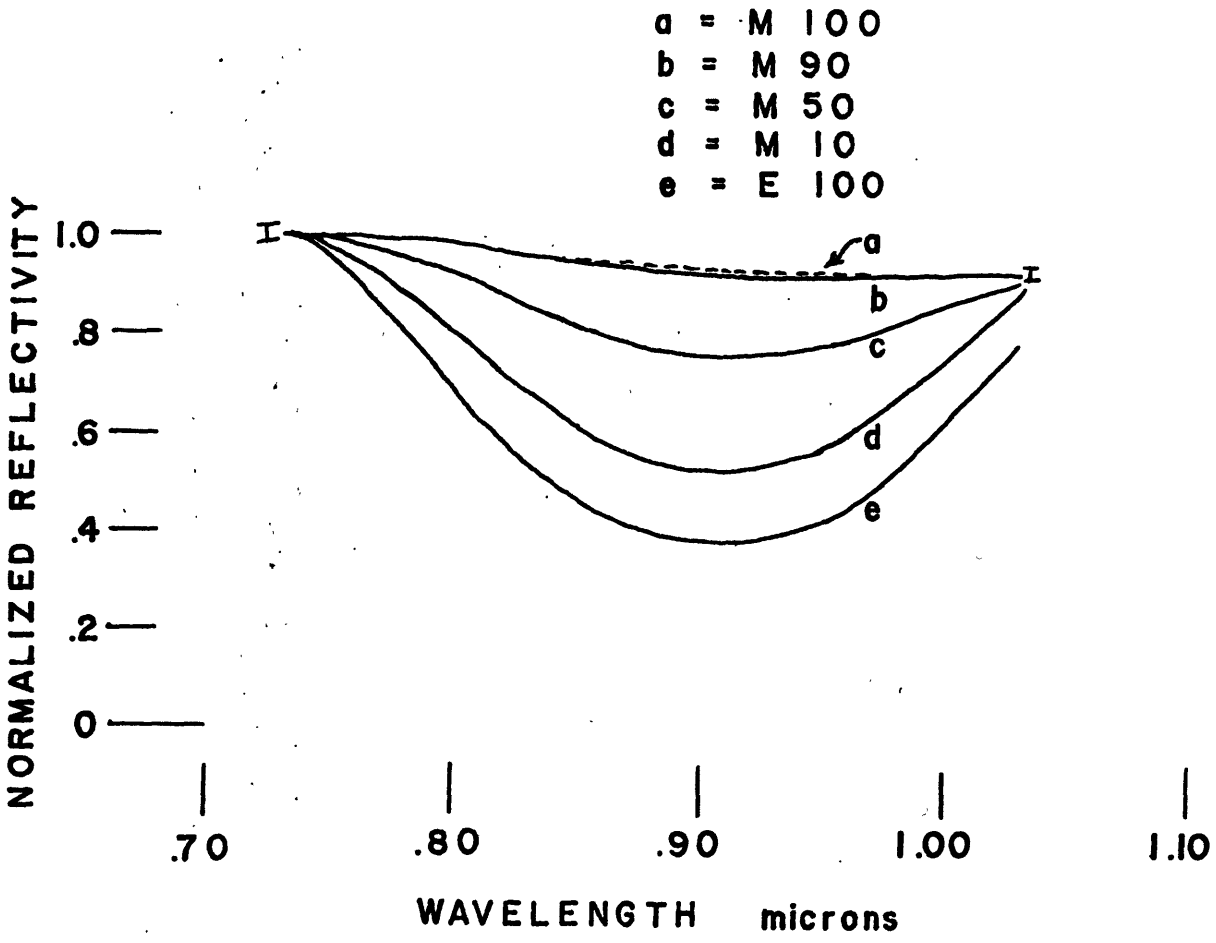

Figure IV.9 Normalized Reflectivity of Enstatite: Magnetite mixtures

of the figures represents the maximum extent of the statistical noise. The maximum noise occurs below .8 microns where the statistics are lowest. The band depth ratio can be read directly from the figures and are also recorded in table IV.1.

With a few notable exceptions, the band depth has decreased for all samples implying a decrease in the total mean optical path length. The first exception, the previously saturated sample E[250,125], provides insight to this change of MOPL. It cannot be simply the addition of more specular component: the MOPL of the diffuse component must be smaller to account for the increase in the band depth. The second exception can be tentatively ignored, for samples Evf and E<63, since there are large differences in sample packing between the two types of measurements which apparently has a stronger effect on the MOPL than the phase does.

POLARIZATION:

Without an exception, the polarization increases in the absorption band. The polarization of the samples are shown in figures IV.10, 11, and 12. Some critical values are listed in table IV.2 for comparison. The only dubious distinction is between M90 and M100 due to statistical noise. The effect is of course strongest in larger particles where the strongest band occurs. The diffuse component of the reflection increases with decreasing particle size.

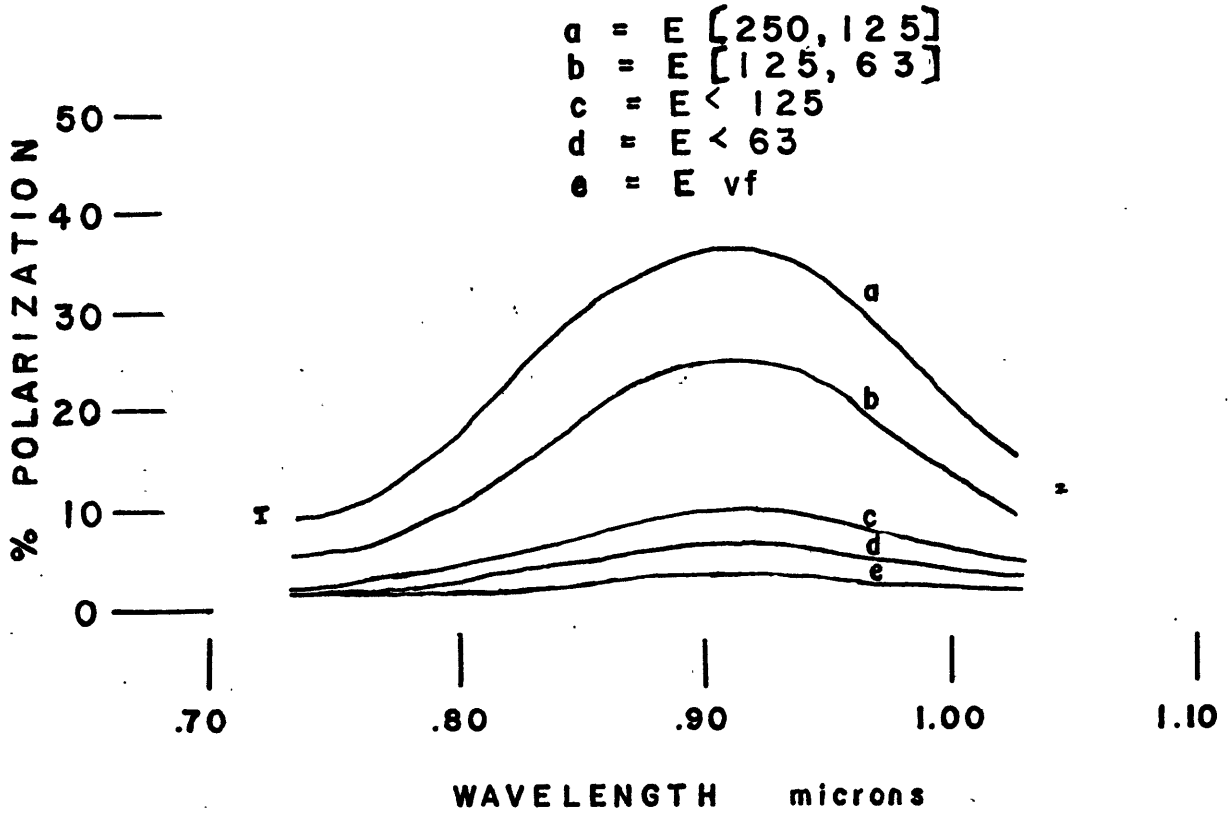

Figure IV.10 Polarization of Enstatite: different particle sizes

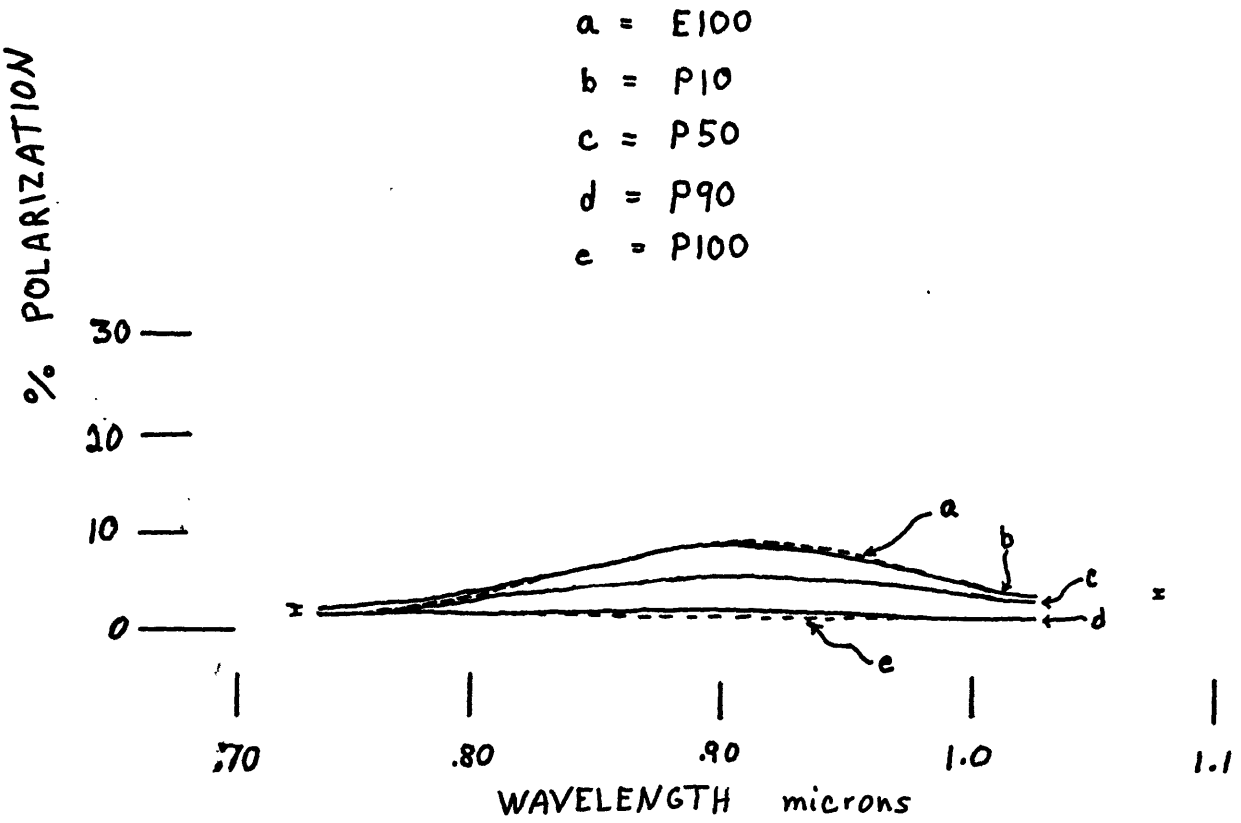

Figure IV.11 Polarization of Enstatite: Plagioclase mixtures

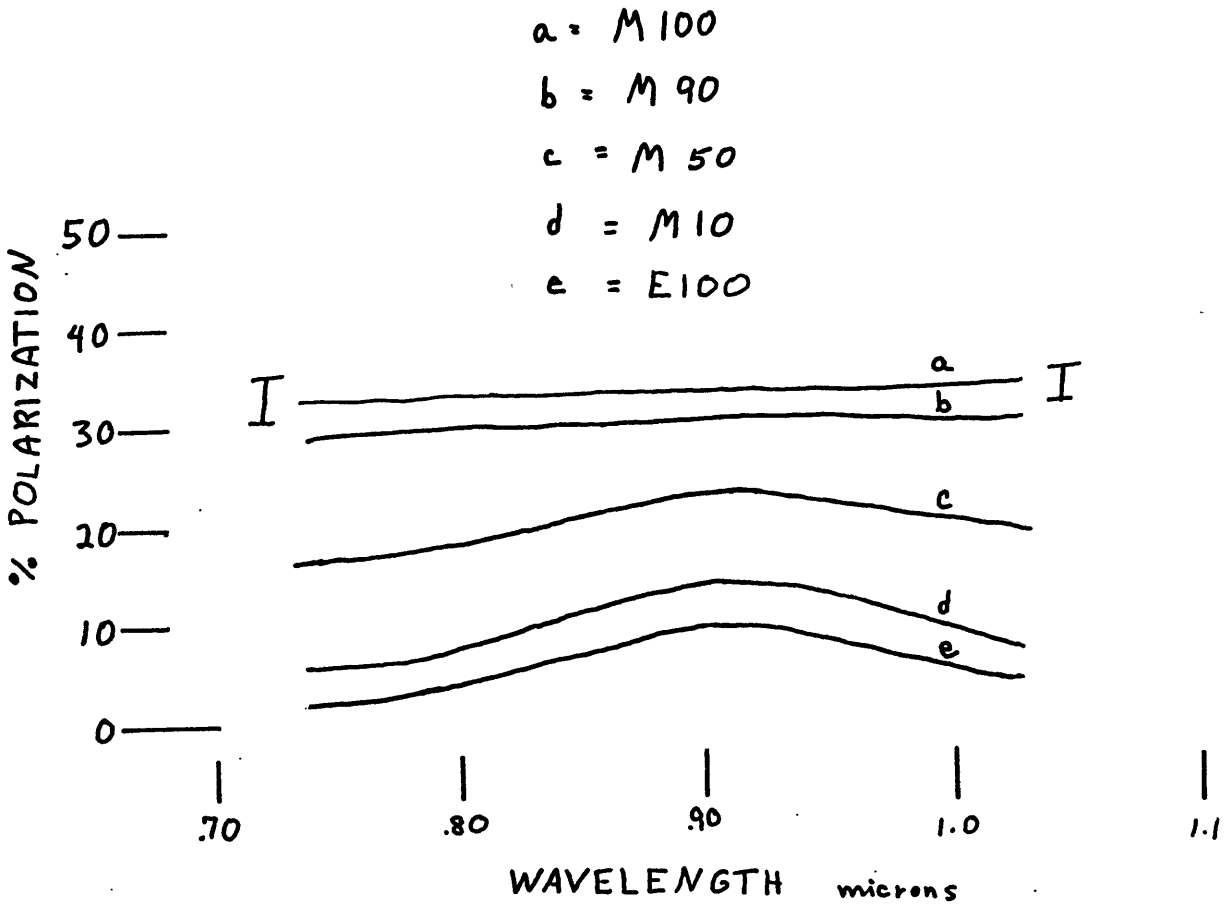

Figure IV.12 Polarization of Enstatite: Magnetite mixtures

Table IV.2 Values of Polarization at 90° Phase

Sample	% Polarization .73 micron	.91 micron	Δ P
E [250,125]	9	36	27
E [125,63]	5.5	24.5	19
E < 125	2	9.5	7.5
E < 63	1.5	6	4.5
Evf	1	3	2
P100	1.75	1.75	-
P90	2	3	1
P50	2.5	6	3.5
P10	2.5	9.5	7
E100	2	9.5	7.5
M10	5.75	14.2	8.45
M50	17	23.5	6.5
M90	29	31	2
M100	32.5	34	1.5

A noteworthy comparison is between the plagioclase mixtures and the magnetite mixtures. The polarization of a constant specular component (Fresnel reflection) causes the polarization for all samples at this phase. For the bright plagioclase mixtures, the ratio of the amount of specular component to the amount of diffuse component is small as indicated by the low polarization. For magnetite, however, the specular/diffuse ratio is larger, and changes of the diffuse component in an absorption band cause a larger magnitude of change in polarization. The significance of this is best visualized by refering to the block diagram of figure IV.13, which shows how the polarization will change for a 25% absorption of the diffuse component for two different cases of original polarization. For small amounts of absorption it is easier to detect polarization differences in material that is already strongly polarized than in a diffuse substance; ie. the magnitude of polarization change is greater for dark material even though the MOPL has been severely reduced.

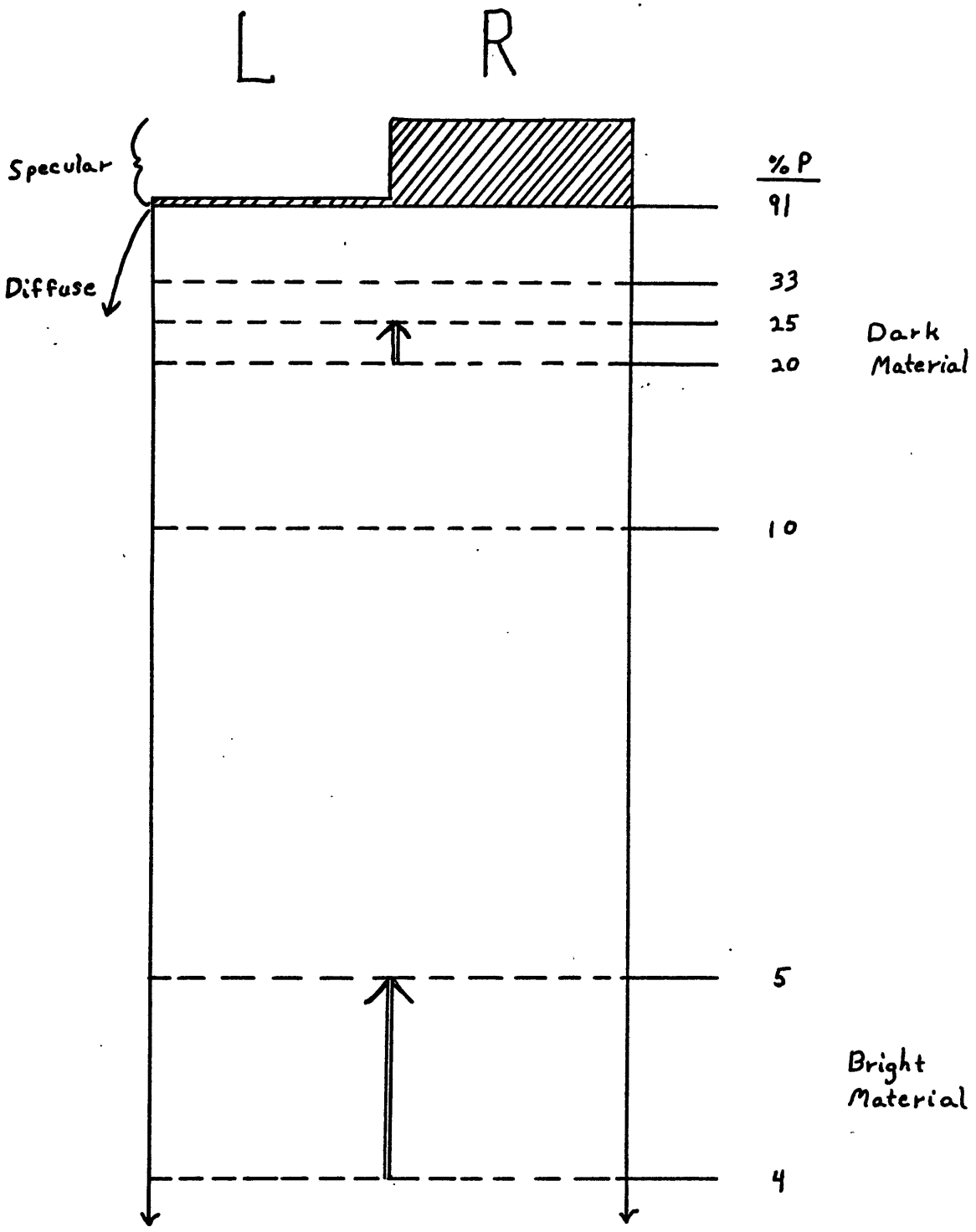

Figure IV.13 The effect of 25% absorption of the diffuse component on the magnitude of polarization. The shaded area corresponds to the magnitude of the specular component. The unshaded area refers to the relative amount of diffuse component.

V. Conclusions

The major conclusion supported by both theoretical and experimental evidence is that when there is significant positive polarization of the light reflected from a particulate surface, the magnitude of the polarization will increase in the spectral region of an absorption band. The amount of change is a function of particle size as well as type and amount of mixture of the absorbing mineral with other minerals. For pure enstatite$_{89}$ samples, the polarization increases three to four fold in an absorption band with the greatest change of magnitude for the larger particles (lower overall reflectivity). The reason for the change of polarization is that the absorption which occurs in the diffuse component changes the ratio of the specular to diffuse components. Both Reflectivity and Polarimetric measurements can detect an absorption band. Mixtures of 50% plagioclase have a magnitude change of polarization of 3.5%, which is a one to two fold increase. Mixtures of 50% magnetite have a change of polarization of 6.5%, which is a 26% increase. For low albedo surfaces expecially, polarimetry may provide a new sensitive tool.

Other conclusions from the theoretical discussion are: 1) The angle of maximum polarization of light reflected from a particulate surface is not an accurate indication of the real refractive index of the surface material. It is a function of the relative portions of diffuse and specular

components of reflection.

2) The variation of the real refractive index in the region of a transition metal absorption band of a mineral has essentially no effect on the reflective properties of the surface.

VI. Applications

Polarimetry can only be applied to a few planetary objects to detect absorption bands. The moon and Mercury are the only planets that can be observed at large phase angles. Mercury has suggestions of absorption bands in its spectrum (McCord in preparation). The most promising application is with the moon, which not only has absorption bands in its spectrum, but has different types resulting from different surface composition of various areas of the moon (recall Adams and McCord 1972).

With the conclusion of the Apollo landing program, earth-based astronomical measurements can be a powerful tool in extending the known results to any location on the front face of the moon. In particular, to determine the composition of the average pyroxene at any location, the methods previously used to detect the absorption bands must be refined to more accurately determine the wavelength of the band center. For reflectivity measurements this requires greater spectral resolution and still involves relative lunar measurements, stellar measurements, and stellar calibrations. For polarimetric measurements the same spectral resolution is required, but each lunar area can be measured independently from all others. The only calibration required is the polarization of the equipment, which can be done by observing known unpolarized stars. Development of the equipment, however, with the proper sensitivity may be the major problem.

APPENDIX A Mean Optical Path Length of Reflection from a Particulate Surface: Order of Magnitude Estimation

Diffuse reflection spectra were made on a Cary 17 spectrometer for samples of various particle sizes of glass. The samples were prepared by crushing ordinary microscope slides whose thickness originally were .001 meter ±5%. Spectra were also taken for a single slide (2 thicknesses) and two slides (4 thicknesses). These spectra are presented in Figures A.1 and A.2. Origin of the absorption band was not investigated. Spectrum a has an optical path length of approximately .002 meters and spectrum b of approximately .004 meters. If the absorption coefficent at 4000Å of a is used to calculate the expected absorption coefficent of b, the observed value is within the errors imposed by the variable thickness of the slides. The particle size for the spectra of figure A.1 are in microns.

From the spectra it can be inferred that:

1) As the particle size is decreased the MOPL is drastically reduced. It seems that very little of the energy loss of spectrum 1 is due to transmission absorption since the absorption band is almost nonexistent. All spectra, therefore, have some constant non-transmission energy loss.

2) By comparing figure A.1 and A.2 one can estimate the MOPL:

Spectrum	Particle size	MOPL
5	1000-500	about .004 meter
4	500-250	between .002 and .004 meter
3	250-125	slightly less than .002 meter.

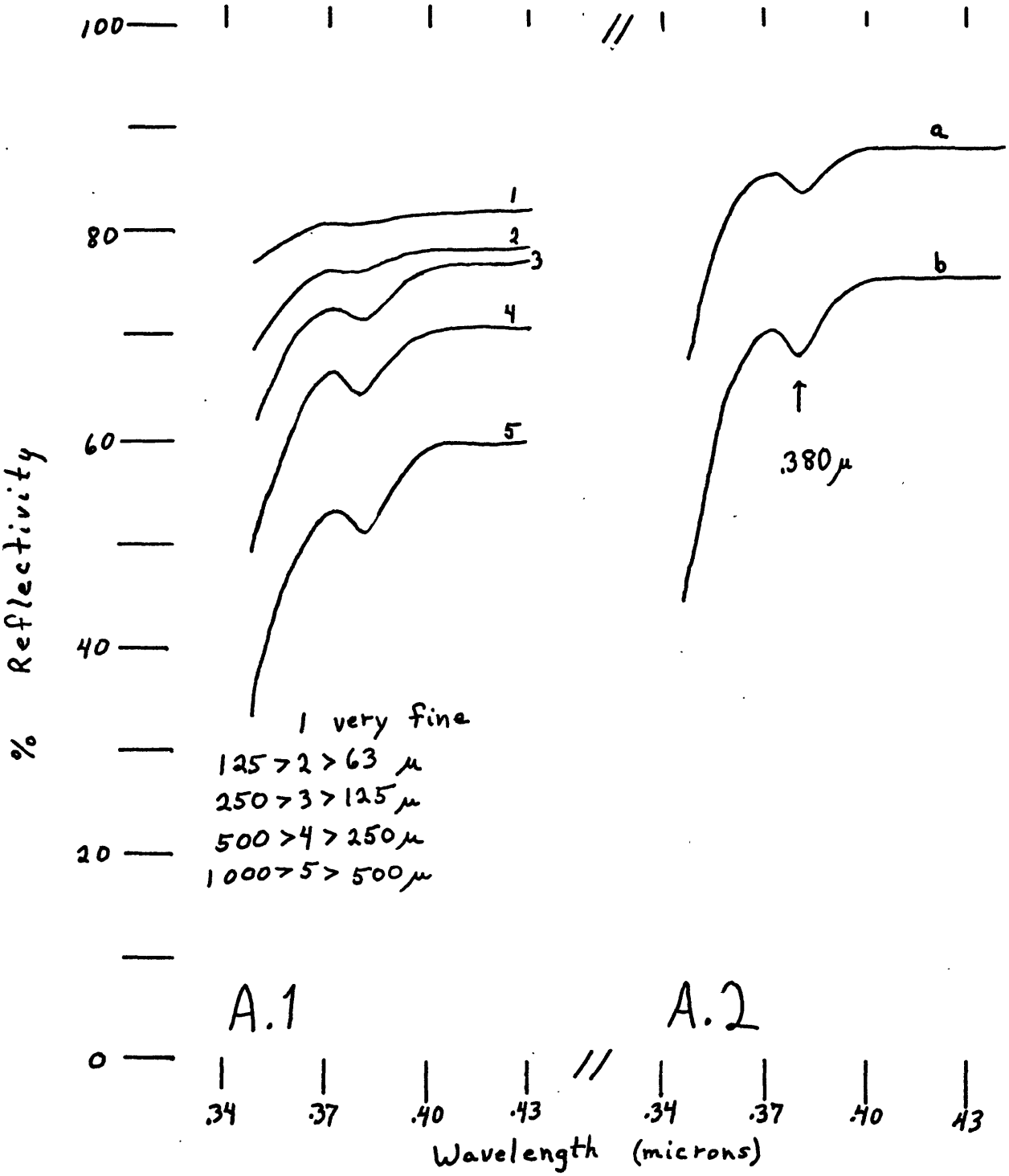

Figure A.1 Diffuse Reflection Spectra of glass of various particle sizes

Figure A.2 Spectra of a) single glass slide, b) double glass slide.

APPENDIX B Polarization of MgO

Polarization measurements at 90° phase from .73 to 1.03 microns were obtained for two different smoked MgO surfaces using the technique described in section IV.C. The results are sumarized as follows:

Sample	%P (.73μ)	%P (1.03μ)
MgO 7-6-72 (3 days old)	4.75	2.8
MgO 7-11-72 (new)	5.5	4.1

For both cases the decrease of polarization with wavelength appears to be linear from .73 to 1.03 micron.

These results are surprising for two reasons:

1) The magnitude of the polarization. MgO is considered as a nearly perfect Lambert surface and therefore should be very close to perfectly diffusing. This is not the case. In fact, many of the bright samples included in this study were better diffusing surfaces (probably due to their hummocky texture).

2) The variation with wavelength. Throughout the polarization studies presented here and elsewhere polarization increases with absorption. This cannot be the cause for the decreasing polarization for MgO. If anything, MgO is brighter at .73μ than at 1.01μ. The variation is not related directly or inversely to the spectrum of the source, which is polarized in a plane perpendicular to that of MgO and all other samples.

The polarization of MgO appears to be real, although unexplained. MgO is NOT an acceptable standard when making

polarization measurements.

References

1. Adams, J.B., Filice, A.L.,1967, "Spectral Reflectance 0.4 to 2.0 Microns of Silicate Rock Powders", JGR 72, No. 22, 5705-5715.

2. Adams, J.B., McCord,T·B., 1971a, "Alteration of Lunar Optical Properties: Age and Composition Effects", Science, 171, 567-571.

3. Adams, J.B., McCord, T.B., 1971b, "Optical Properties of Mineral Separates, Glass, and Anorthositic Fragments from Apollo Mare Samples", Geochim. Cosmochim. Acta.

4. Adams, J.B., McCord, T.B., 1972, "Electronic Spectra of Pyroxenes and Interpretation of Telescopic Spectral Reflectivity Curves of the Moon", Proc. of Third Lunar Science Conf., in press.

5. Bancroft, G.M., Burns, R.G., 1967, "Interpretation of the Electronic Spectra of Iron in Pyroxenes", Am. Min., 52: 1278-1287.

6. Born, Max, Wolf, Emil, Principles of Optics, Pergamon Press, 1964.

7. Burns, R.G., Mineralogical Applications of Crystal Field Theory, Cambridge University Press, London, 1970.

8. Dollfus, A., 1961, "Polarization Studies of Planets", Planets and Satellites, U. of Chicago Press.

9. Dollfus, A., Bowell, E., Titulaer, C., 1971, "Polarimetric Properties of the Lunar Surface and its Interpretation, Parts I, II, and III", Astron. and Astrophys., 10, 29-53; 10, 450-466; 12, 199-209.

10. Fowles, G.R., Introduction to Modern Optics, Holt, Reinehart and Winston, Inc., 1968.

11. Garbuny, Max, Optical Physics, Academic Press, New York, 1965.

12. Gehrels, T., Teska, T.M., 1963, "The Wavelength Dependence of Polarization", Applied Optics, Vol. 2, No. 1, 67-76.

13. Gehrels, T., Coffeen, T., Owings, D., 1964, "Wavelength Dependence of Polarization III, The Lunar Surface", Astr. J. Vol 69, No. 10, 826-852.

14. McCord, T.B., 1968, "Time Dependence of Lunar Differential Color", Astron. Journal, 74, No. 2, 273-277.

15. McCord, T.B., Charette, M.P., Johnson, T.V., Lebofsky, L.A., Pieters, C., and Adams, J.B., 1972, "Lunar Spectral Types", JGR, Vol. 77, 1349-1359.

16. Pellicori, S.F., 1969, "Polarizing Properties of Pulverized Materials: Applications to the Lunar Surface", Optical Sciences Center Technical Report 42, Tuscon, Arizona.